BUPT University of Posts and Telecommunications

Open Lecture 5 – Channel Modeling
23 February 2023

Recent Progress on Channel Measurement and Modeling for 6G

Jianhua Zhang

National Key Lab of Network and Switching,

Beijing University of Posts and Telecommunications

Beijing, China

E-mail: jhzhang@bupt.edu.cn

Outline

I. Trend and vision to 6G channel model

II. Our recent progress on 6G channel research

- Terahertz channel measurement and modeling
- Joint communication and sensing channel measurements and modeling
- Massive MIMO channel measurements and modeling
- Intelligent channel modeling and channel prediction

III. Work on 6G channel model standardization

Research trend of mobile communication channel

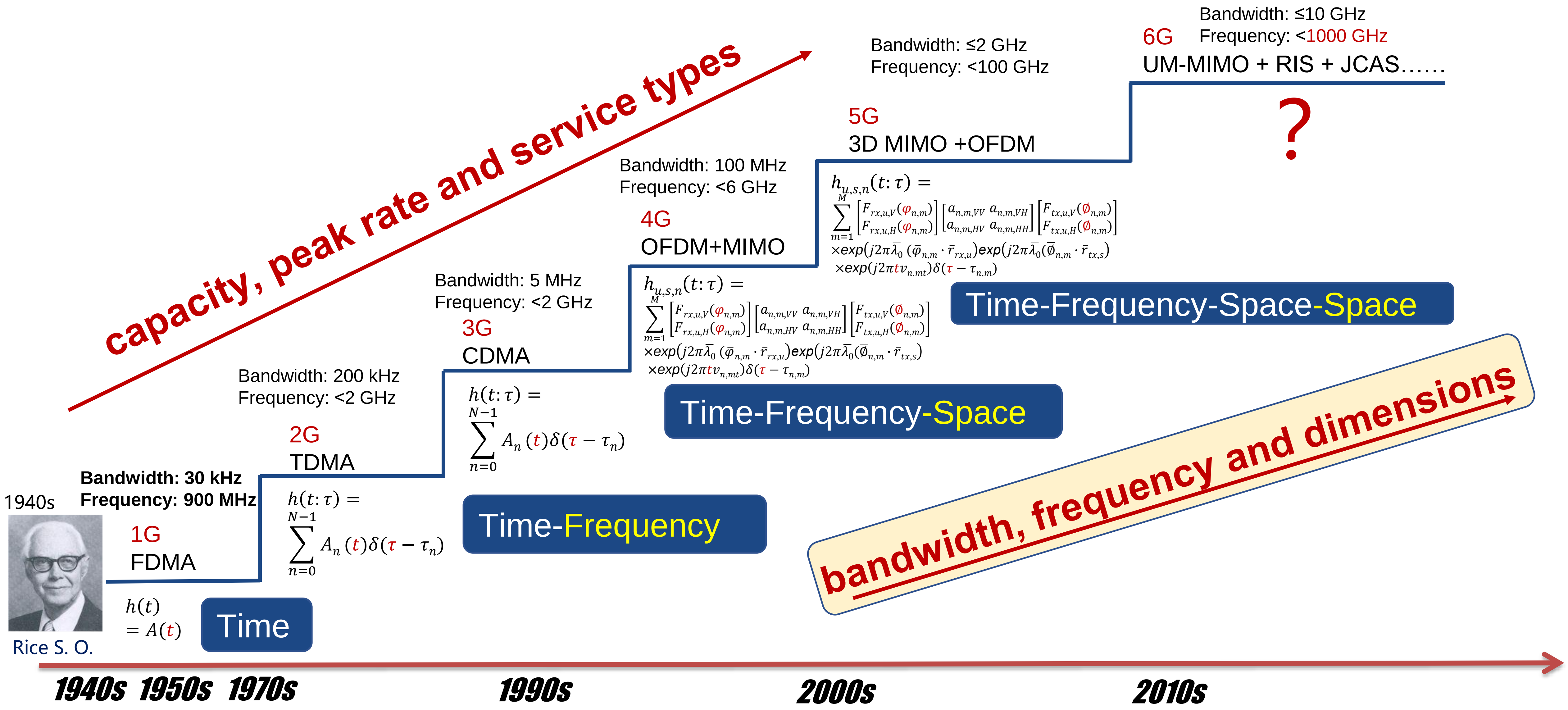

- J. Zhang et al., "Channel Measurements and Models for 6G: Current Status and Future Outlook," *Frontiers of Information Technology & Electronic Engineering, 2020.*

Research trend of mobile communication channel

4G
OFDM+MIMO

5G
OFDM+3D MIMO

ITU-R IMT-2020 channel model
DG chairwoman

2D GBSM model

$$h_{u,s,n}(t:\tau) = \sum_{m=1}^{M} \begin{bmatrix} F_{rx,u,V}(\phi_{Rx,l,m}) \\ F_{rx,u,H}(\phi_{Rx,l,m}) \end{bmatrix} \begin{bmatrix} a_{n,m,VV} & a_{n,m,VH} \\ a_{n,m,HV} & a_{n,m,HH} \end{bmatrix} \begin{bmatrix} F_{tx,u,V}(\phi_{Tx,l,m}) \\ F_{tx,u,H}(\phi_{Tx,l,m}) \end{bmatrix}$$
$$\times exp(j2\pi\bar{\lambda}_0 (\bar{\varphi}_{l,m} \cdot \bar{r}_{rx,u}) exp(j2\pi\bar{\lambda}_0(\bar{\varnothing}_{l,m} \cdot \bar{r}_{tx,s})$$
$$\times exp(j2\pi t v_{l,mt})\delta(\tau - \tau_{l,m})$$

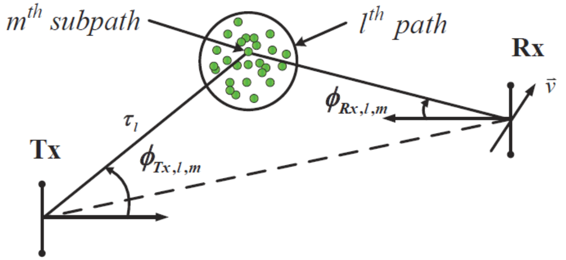

Mandatary:
3D GBSM model

$$h_{u,s,n}(t:\tau) = \sum_{m=1}^{M} \begin{bmatrix} F_{rx,u,V}(\phi_{Rx,l,m}, \theta_{Rx,l,m}) \\ F_{rx,u,H}(\phi_{Rx,l,m}, \theta_{Rx,l,m}) \end{bmatrix} \begin{bmatrix} a_{n,m,VV} & a_{n,m,VH} \\ a_{n,m,HV} & a_{n,m,HH} \end{bmatrix} \begin{bmatrix} F_{tx,u,V}(\phi_{Tx,l,m}, \theta_{Tx,l,m}) \\ F_{tx,u,V}(\phi_{Tx,l,m}, \theta_{Tx,l,m}) \end{bmatrix}$$
$$\times exp(j2\pi\bar{\lambda}_0 (\bar{\varphi}_{l,m} \cdot \bar{r}_{rx,u}) exp(j2\pi\bar{\lambda}_0(\bar{\varnothing}_{l,m} \cdot \bar{r}_{tx,s})$$
$$\times exp(j2\pi t v_{l,mt})\delta(\tau - \tau_{l,m})$$

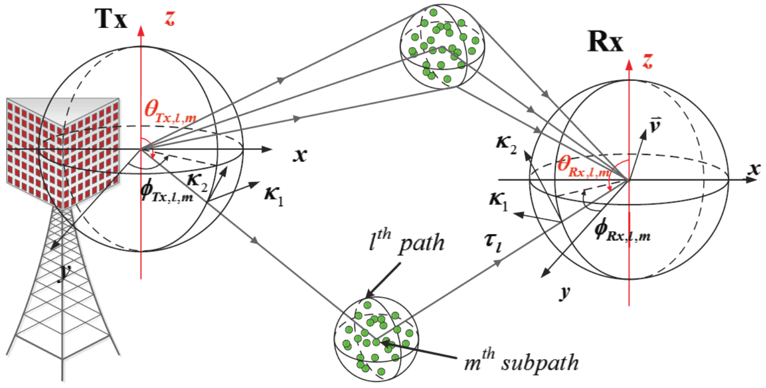

Optional:
Raytracing / Hybrid model

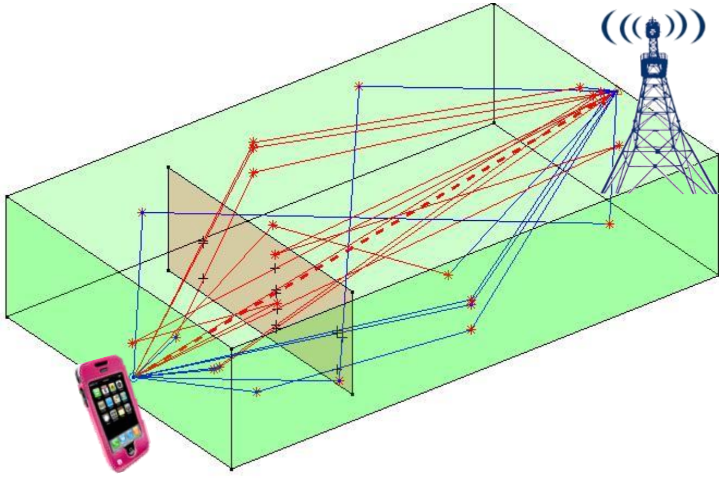

- J. Zhang et al., "3D MIMO: How Much Does It Meet Our Expectation Observed from Antenna Channel Measurements?", IEEE Journal on Selected Areas in Communications, 2017.
- ITU-R M.2412, Guidelines for Evaluation of Radio Interface Technologies for IMT-2020. [R]., 2017

6G channel model vision

- Compared with the 5G channel model, the 6G channel model continues to expand in frequency, bandwidth, application scenario, support technology, etc.

	5G	6G
Frequency	0.5-100 GHz	0.5-1000 GHz
Bandwidth	<2 GHz	< 10 GHz
Application scenario	Indoor, UMi, UMa, RMa	Indoor, UMi, UMa, RMa、IIoT, SGIN, Ultra high-speed mobile
Support technology	3D MIMO, Massive MIMO	3D MIMO, Massive MIMO, Terahertz communication, joint communication and sensing, reconfigurable intelligent surface, holographic communication, space-air-ground integrated network

Outline

I. Trend and vision to 6G channel model

II. Our recent progress on 6G channel research

- Terahertz channel measurement and modeling
- Joint communication and sensing channel measurements and modeling
- Massive MIMO channel measurements and modeling
- Intelligent channel modeling and channel prediction

III. Work on 6G channel model standardization

1.1 Path loss modeling in THz bands

- Proposing 220-330 GHz multi-frequency path loss model to characterize frequency dependence over the large-bandwidth in THz bands.

Frequency dependence

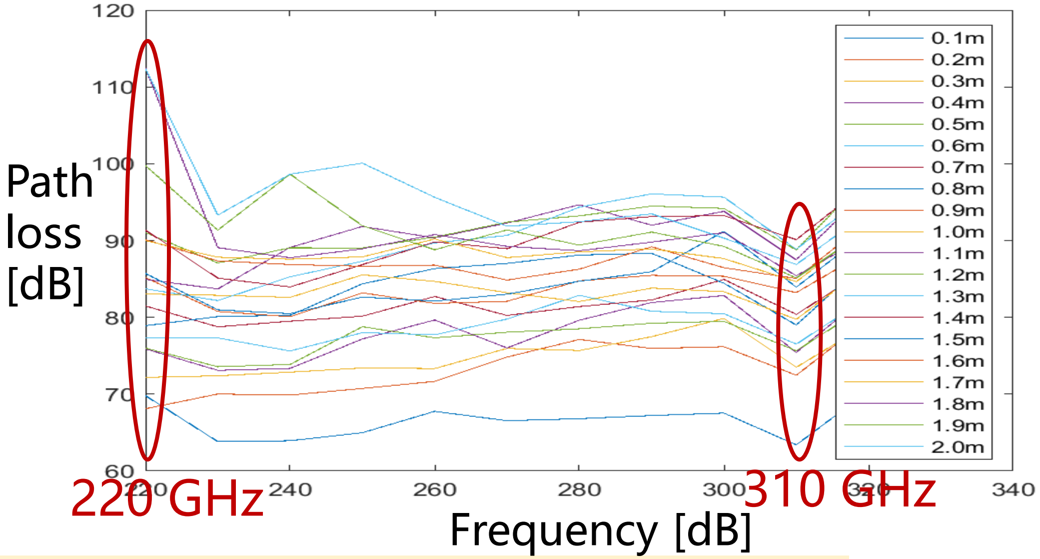

ABG model fitting

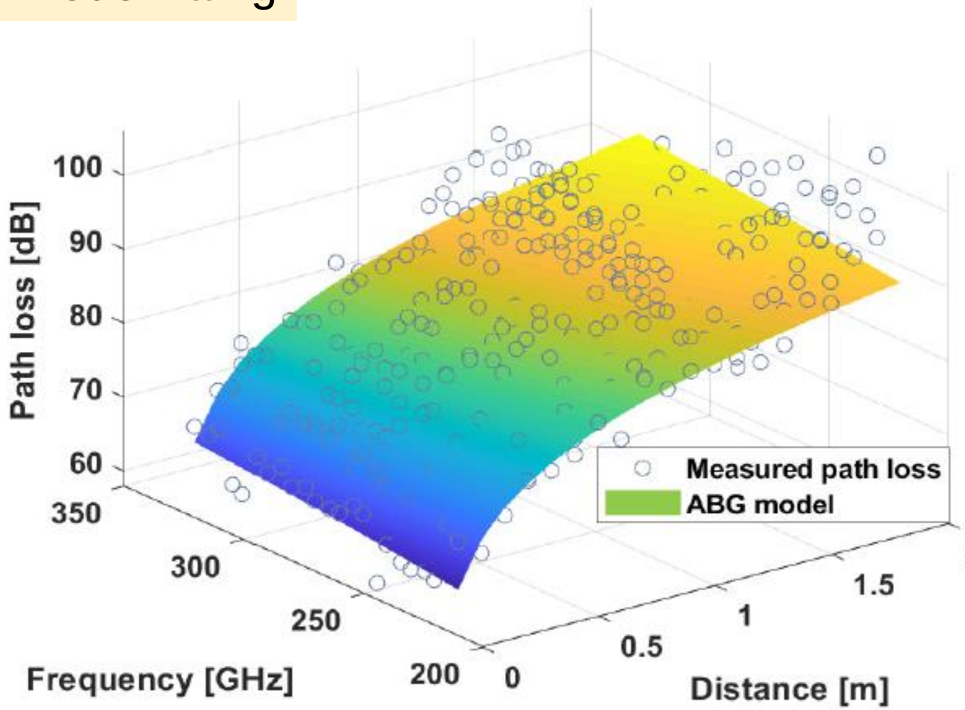

ABG multi-frequency path loss model

$$PL_{ABG}(f,d)[dB] = 19.3\log_{10}\left(\frac{d}{d_0}\right) + 13.27 + 21\log_{10}\left(\frac{f}{1\ GHz}\right) + X_{\sigma=3.78}^{ABG}$$

Frequency dependence factor:
2.1 [ABG model]>2 [Free space path loss model]

- P. Tang, J. Zhang, et.al., "Channel Measurement and Path Loss Modeling from 220 GHz to 330 GHz for short-range wireless communications", China Communications, 2021.

1.2 Reflection coefficient modeling in THz bands

- Proposing the frequency-angle two-dimensional reflection coefficient model to break the restriction of unknown permittivity in THz reflection coefficient modeling.

Measurement scenario

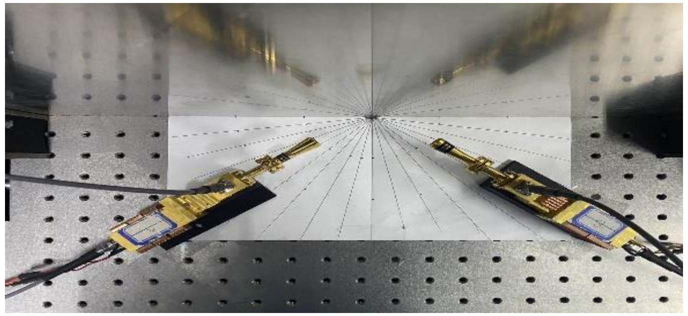

Model fitting

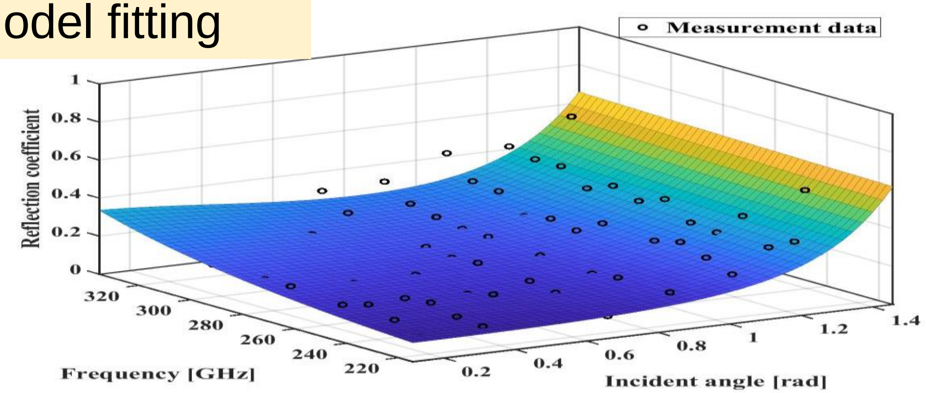

Frequency-angle reflection coefficient model

$$\rho(f,\theta) = e^{-10^{a} f^{2} cos^{2}\theta}\left(\frac{cos\,\theta - \sqrt{1 + \frac{10^{b}}{10^{c} - df^{2} - jf} - sin^{2}\theta}}{cos\,\theta + \sqrt{1 + \frac{10^{b}}{10^{c} - df^{2} - jf} - sin^{2}\theta}}\right)$$

Frequency (f), Angle (θ)

Material	a	b	c	d	RMSE
Glass	-15.45	3.93	3.97	0.06	0.11
Tile	-15.18	3.96	3.72	0.02	0.12
Plasterboard	-15.66	3.57	4.33	0.10	0.08
Board	-15.30	3.89	4.04	0.03	0.10

Small RMSE represents the model fit well

- *Z. Chang, J. Zhang, et.al., "Frequency-Angle Two-Dimensional Reflection Coefficient Modeling Based on Terahertz Channel Measurement," Frontiers of Information Technology & Electronic Engineering, accepted.*

1.3 THz channel parameters

- 3GPP channel model parameters for the indoor hotspot scenario in THz bands are extracted.

Measurement in indoor office scenario

Measurement in urban microcellular scenario

Channel parameters

Scenarios		Office LOS (100 GHz)	Office NLOS (100 GHz)	UMi LOS (132 GHz)	UMi NLOS (132 GHz)
Path loss (CI model)	PLE	1.94	2.78	2.16	2.44
Delay spread (DS) lgDS=log10(DS/1s)	m_{lgDS}	-8.82	-8.10	-8.05	-8.53
	s_{lgDS}	0.16	0.16	0.46	0.18
AOA spread(ASA) lgASA=log10(ASA/1°)	m_{lgASA}	1.37	1.62	1.26	1.76
	s_{lgASA}	0.21	0.11	0.42	0.15
Shadow fading (SF) [dB]	s_{SF}	2.77	6.00	5.26	5.88
K-factor(K) [dB]	m_K	10.01	-	14.57	-
Number of clusters		4	5	4	3
Number of rays per cluster		3	5	4	2
Cluster DS (C_{DS}) in [ns]		0.5	1.4	6.4	0.3
Cluster ASA (C_{ASA}) in [deg]		1.5	4.7	0.8	0.6
Cross-Correlations	ASA vs DS	0.10	0.33	0.30	0.37
	ASA vs SF	0.38	-0.57	0.04	0.35
	DS vs SF	0.47	-0.49	0.04	0.59
	ASA vs K	0.05	-	-0.61	-
	SF vs K	0.67	-	-0.54	-
	DS vs K	-0.32	-	-0.33	-
Correlation distance in the horizontal plane [m]	ASA	2.1	2.4	10.6	5.7
	DS	1.9	1.0	8.3	5.1
	SF	2.0	0.8	9.0	7.5
	K	2.4		5.0	

- *ITU-R Document 5D/1640-E, "Proposal on the Development of Preliminary Draft New Report," 43th Meeting of Working Party 5D, E-Meeting, 2023.*

1.4 THz channel modeling

- Deterministic ray tracing is a promising approach to THz channel modeling in 6G deployment scenarios.

THz Channel Characteristics

- High Propagation Loss
- Sparsity
- Near-Field and Spatial Non-Stationarity

RT Simulation Characteristics

- High scalability
- Known environmental database

In THz bands, there is a lack of complete knowledge of material EM properties.

- High complexity

Due to the sparsity of THz channel, it is possible to simulate the dominant path with lower complexity.

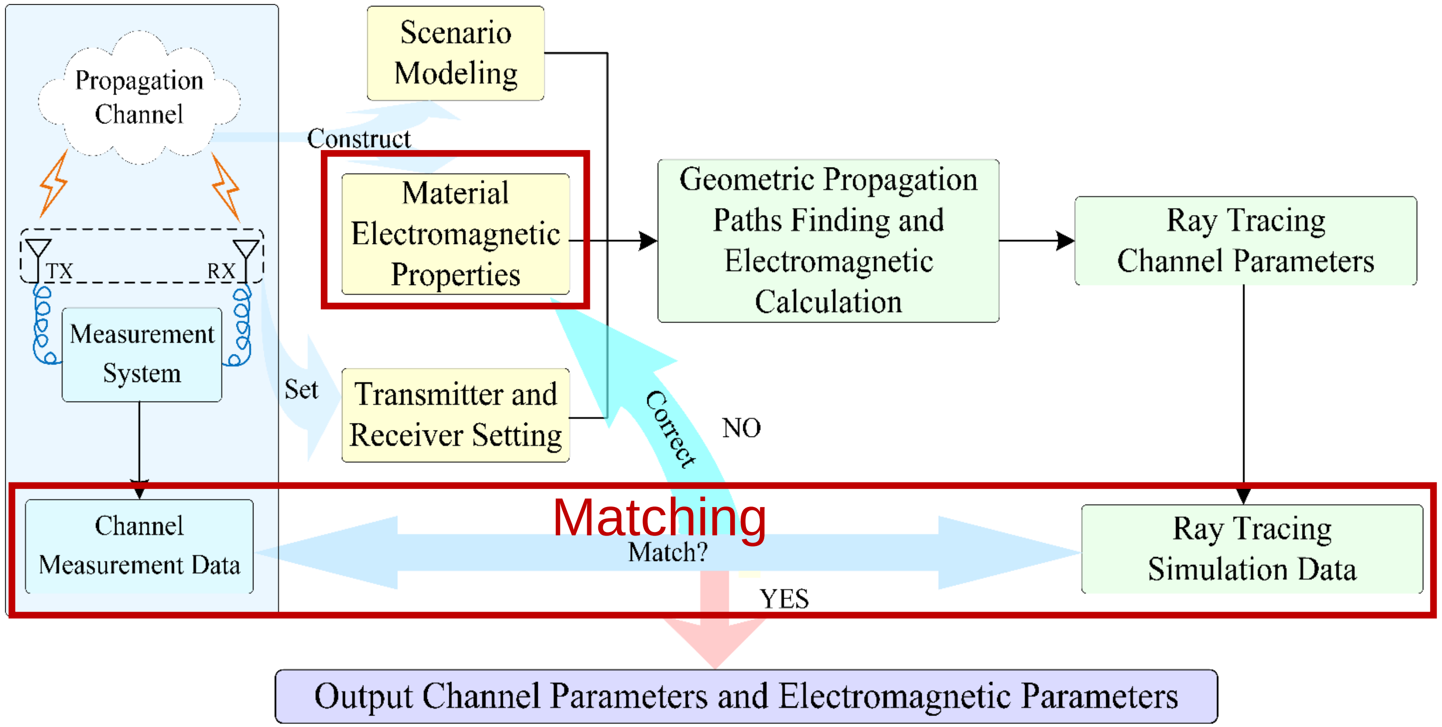

RT simulation process based on measured calibration

- J. Zhang, J. Lin, P. Tang, W. Fan, X. Liu, Z. Yuan, H. Xu, Y. Lyu, L. Tian and P. Zhang, "Deterministic Ray Tracing: A Promising Approach to THz Channel Modeling in 6G Deployment Scenarios," IEEE Communications Magazine, accepted.

1.4 THz channel modeling

- The comparison of measurement and RT results shows that the method can accurately describe the THz channel characteristics.

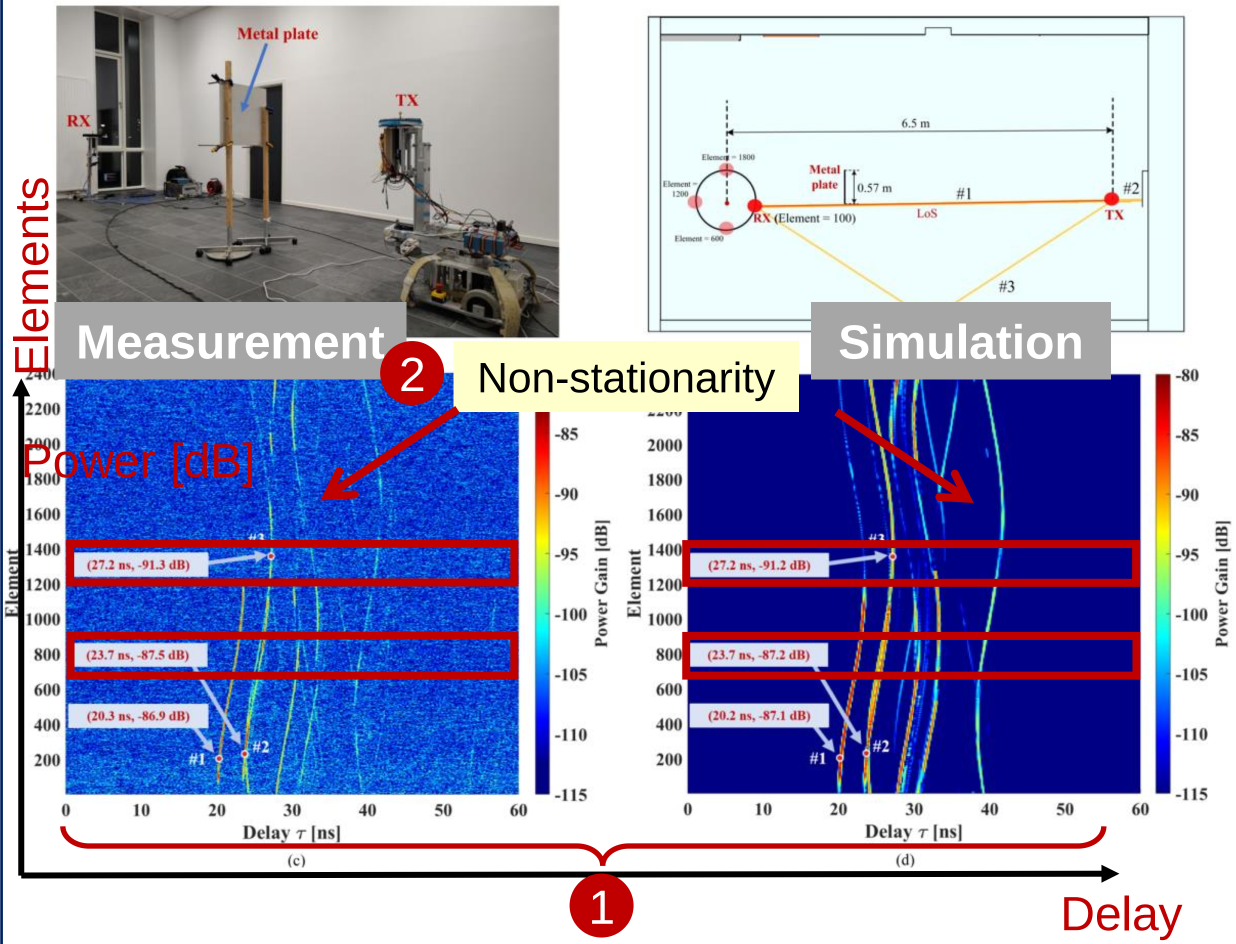

Path	Parameter	Measure-ment	RT	Deviation
#1	Delay (ns)	20.3	20.2	0.1
	Power (dB)	-86.9	-87.1	0.2
#2	Delay (ns)	23.7	23.7	0
	Power (dB)	–87.5	–87.2	-0.3
#3	Delay (ns)	27.2	27.2	0
	Power (dB)	–91.3	–91.2	-0.1

1 Good consistency between the actual measurement and RT simulation in multipath delay and power.

2 Accurate simulation for the channel spatial non-stationarity by RT.

- *J. Zhang, J. Lin, P. Tang, W. Fan, X. Liu, Z. Yuan, H. Xu, Y. Lyu, L. Tian and P. Zhang, "Deterministic Ray Tracing: A Promising Approach to THz Channel Modeling in 6G Deployment Scenarios," IEEE Communications Magazine, accepted.*

1.5 Channel sparsity

- The channel sparsity is verified experimentally in sub-THz, mm-wave, and cm-wave bands.

Measurement scenarios and system

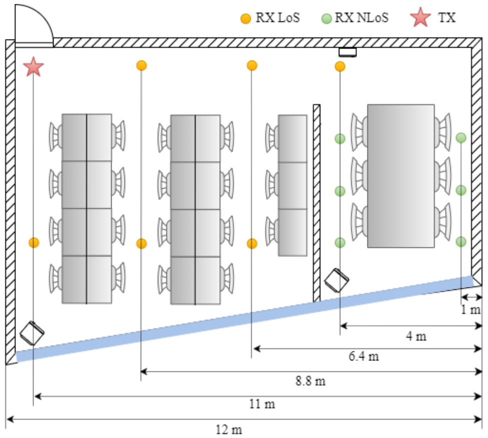

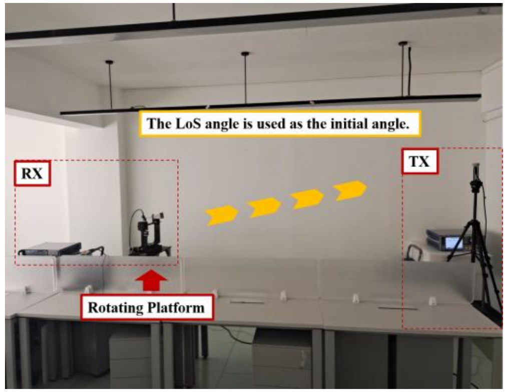

Parameters	cmWave	mmWave	sub-THz
Carrier frequency	6 GHz	26 GHz	132 GHz
TX antenna	Omnidirectional antenna with fixed position		Directional antenna
RX antenna	Horn antenna rotating in 10° steps		

Sparsity comparison

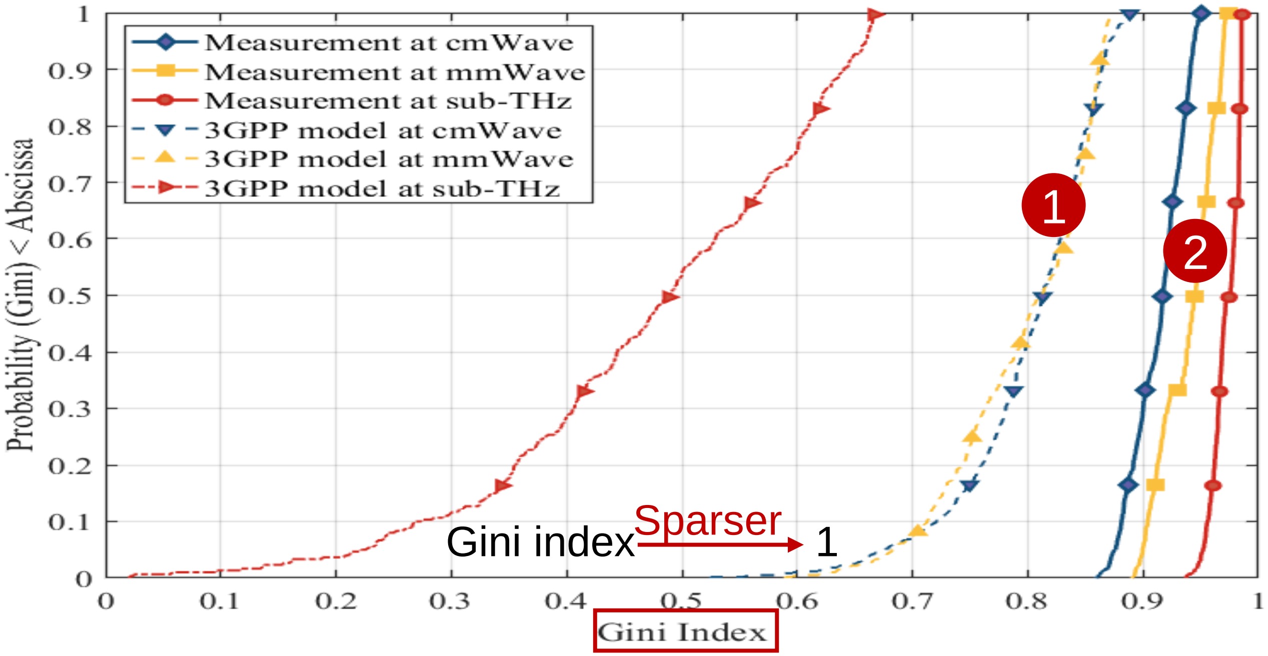

1. The 3GPP model fails to characterizing sparsity.
2. Sparsity: sub-THz > mm-wave > cm-wave

- X. Liu, J. Zhang, P. Tang, L. Tian, H. Tataria, S. Sun, M. Shafi , “Channel Sparsity Variation and Model-Based Analysis on 6, 26, and 132 GHz Measurements”, arXiv preprint arXiv: 2302.08772 , 2023.

1.5 Channel sparsity

- The intra-cluster power allocation model is proposed to enable the 3GPP channel model to characterize sparsity in the delay domain.

Intra-cluster power allocation model

Proposed new parameter: intra-cluster K-factor

$$I = \frac{\max(\mathbf{p}_n)}{\|\mathbf{p}_n\|_1 - \max(\mathbf{p}_n)}$$

The power vector of all rays within the n-th cluster

The channel coefficients of the n-th cluster

$$H_n(t) = \sqrt{\frac{I}{I+1} \cdot P_n} \cdot c_1 \exp(j2\pi v_1 t) + \sqrt{\frac{1}{I+1} \cdot \frac{P_n}{M-1}} \cdot \sum_{m=2}^{M} c_m \exp(j2\pi v_m t)$$

The n-th cluster power

The rays number within a cluster

Sparsity comparison

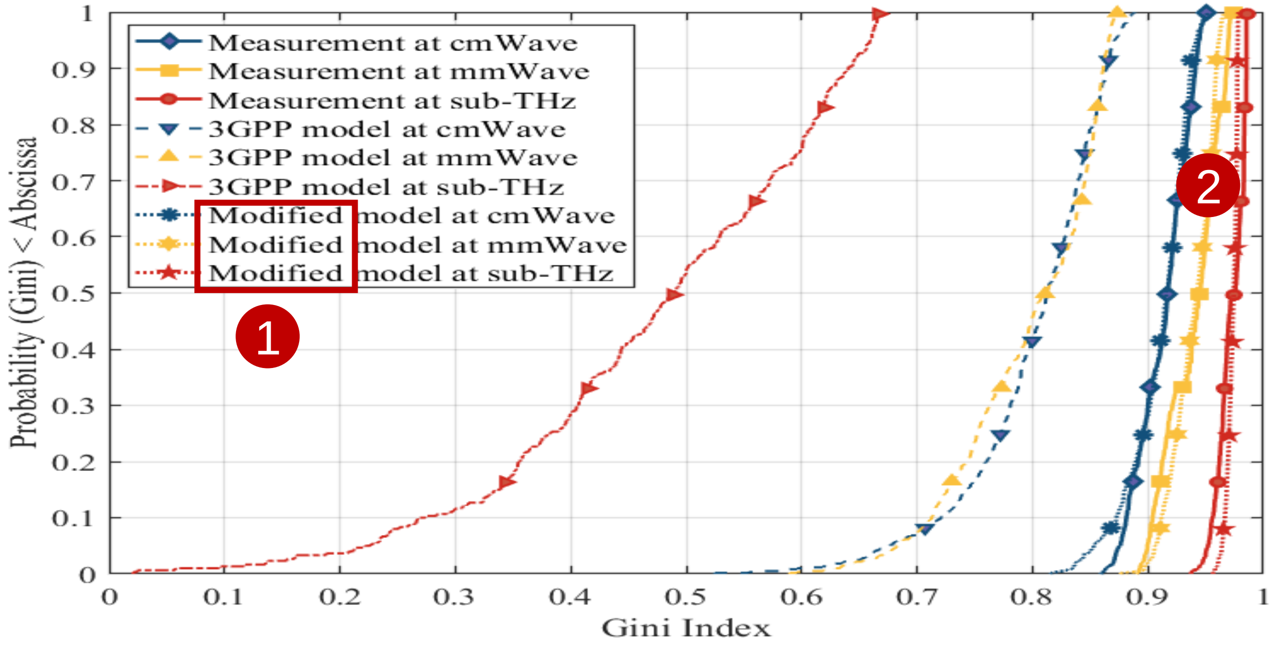

1. Modifying 3GPP model by Intra-cluster power allocation model.
2. Modified model characterizes measurement sparsity well.

- *X. Liu, J. Zhang, P. Tang, L. Tian, H. Tataria, S. Sun, M. Shafi , "Channel Sparsity Variation and Model-Based Analysis on 6, 26, and 132 GHz Measurements", arXiv preprint arXiv: 2302.08772 , 2023.*

Outline

I. Trend and vision to 6G channel model

II. Our recent progress on 6G channel research

- Terahertz channel measurement and modeling
- Joint communication and sensing channel measurements and modeling
- Massive MIMO channel measurements and modeling
- Intelligent channel modeling and channel prediction

III. Work on 6G channel model standardization

2.1 Environment effects on sensing channel characteristics

- Based on the CIR correlation between sensing target and interference, environment effects on sensing channel characteristics are analyzed.

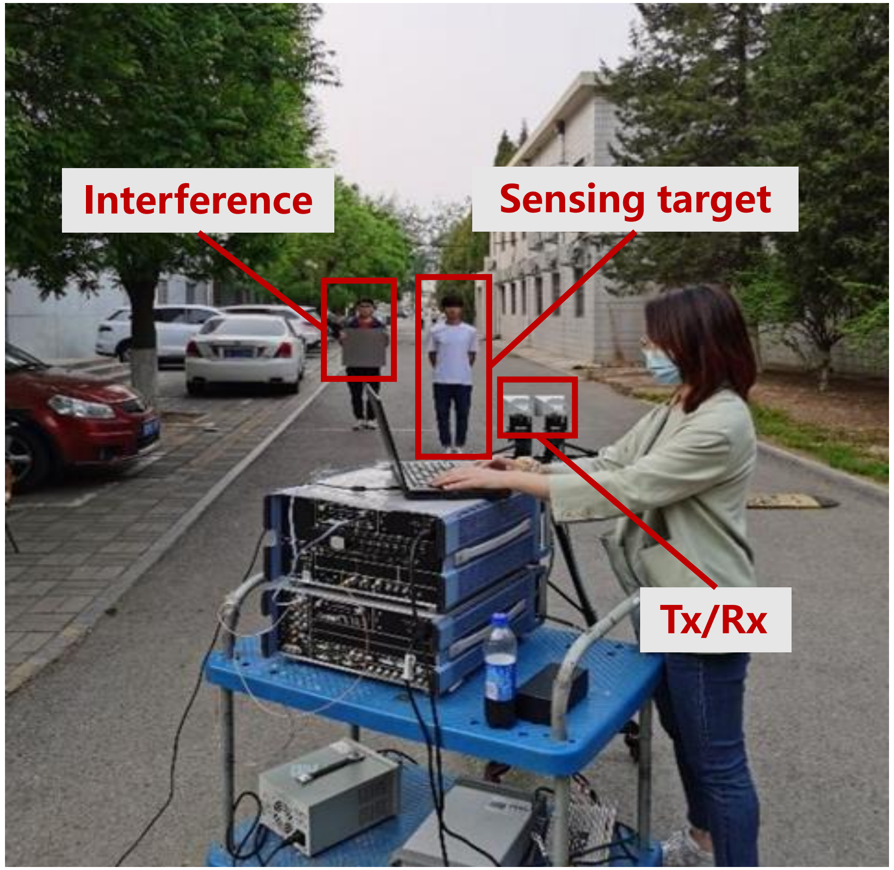

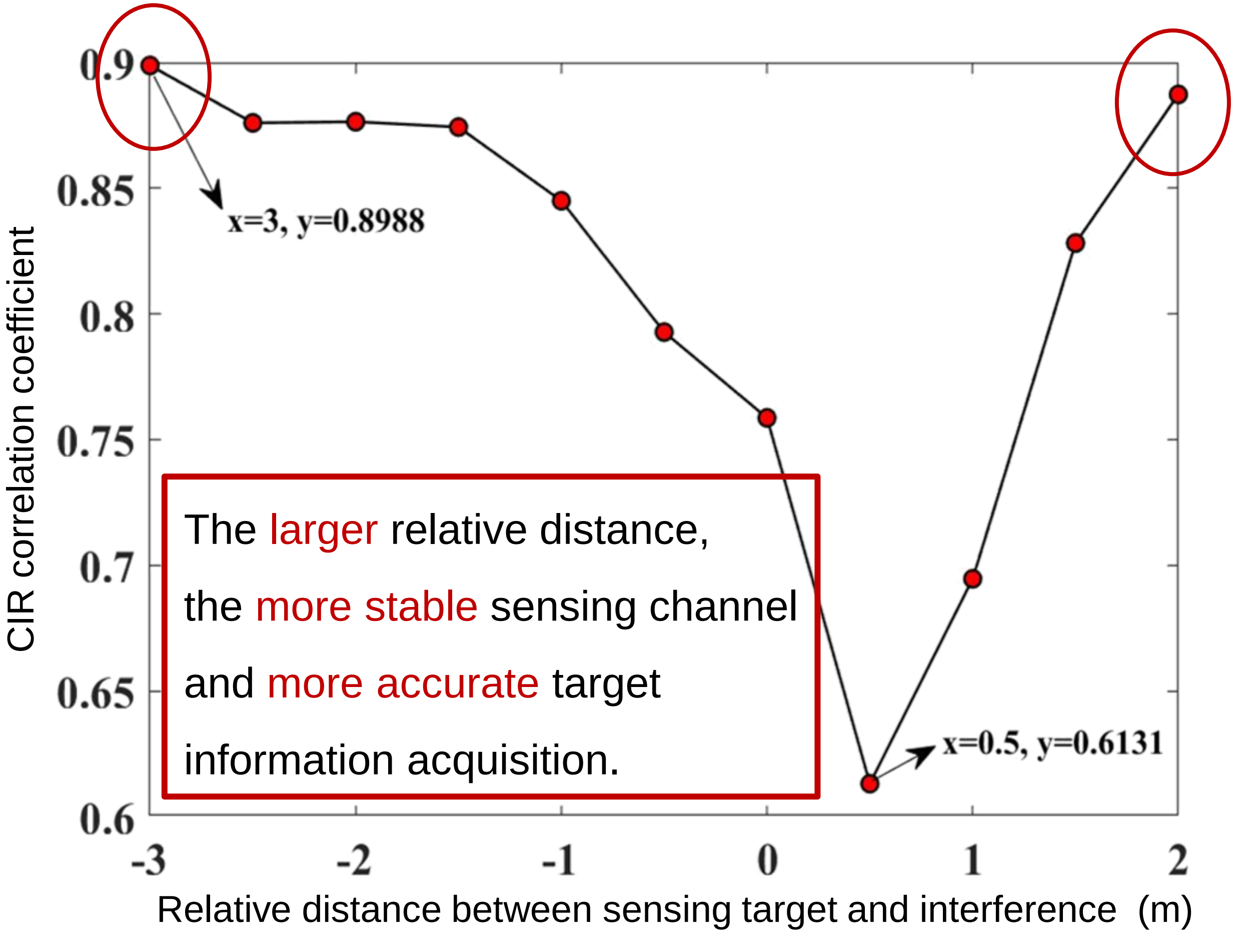

- *J. Wang, J. Zhang, Y. Zhang et al., "Empirical Analysis of Sensing Channel Characteristics and Environment Effects at 28 GHz," IEEE GLOBECOM Workshops, 2022.*

2.2 Small-scale fading modeling in JCAS channel

- The shared scatterers by JCAS channels are observed based on channel measurements.

Measurement scenarios

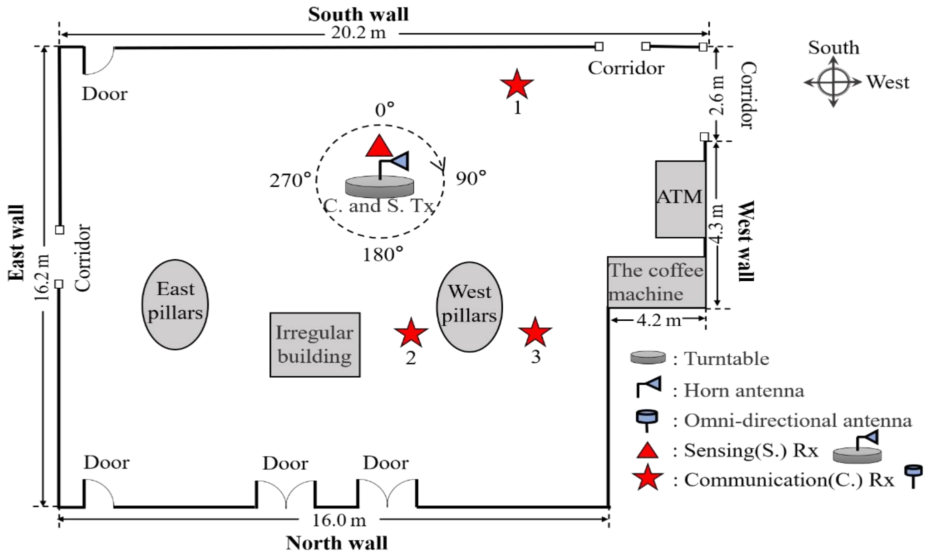

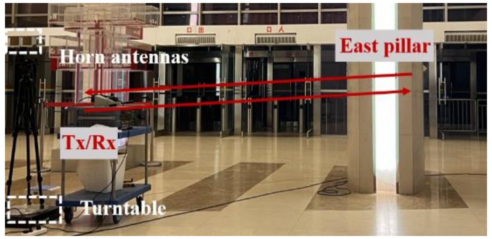

The sensing scenario

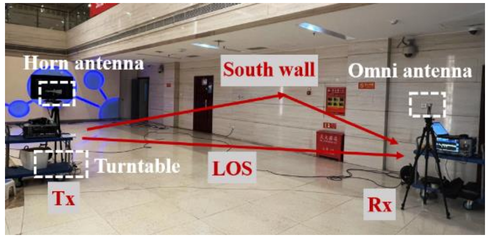

The communication scenario

Power-angular-delay profiles

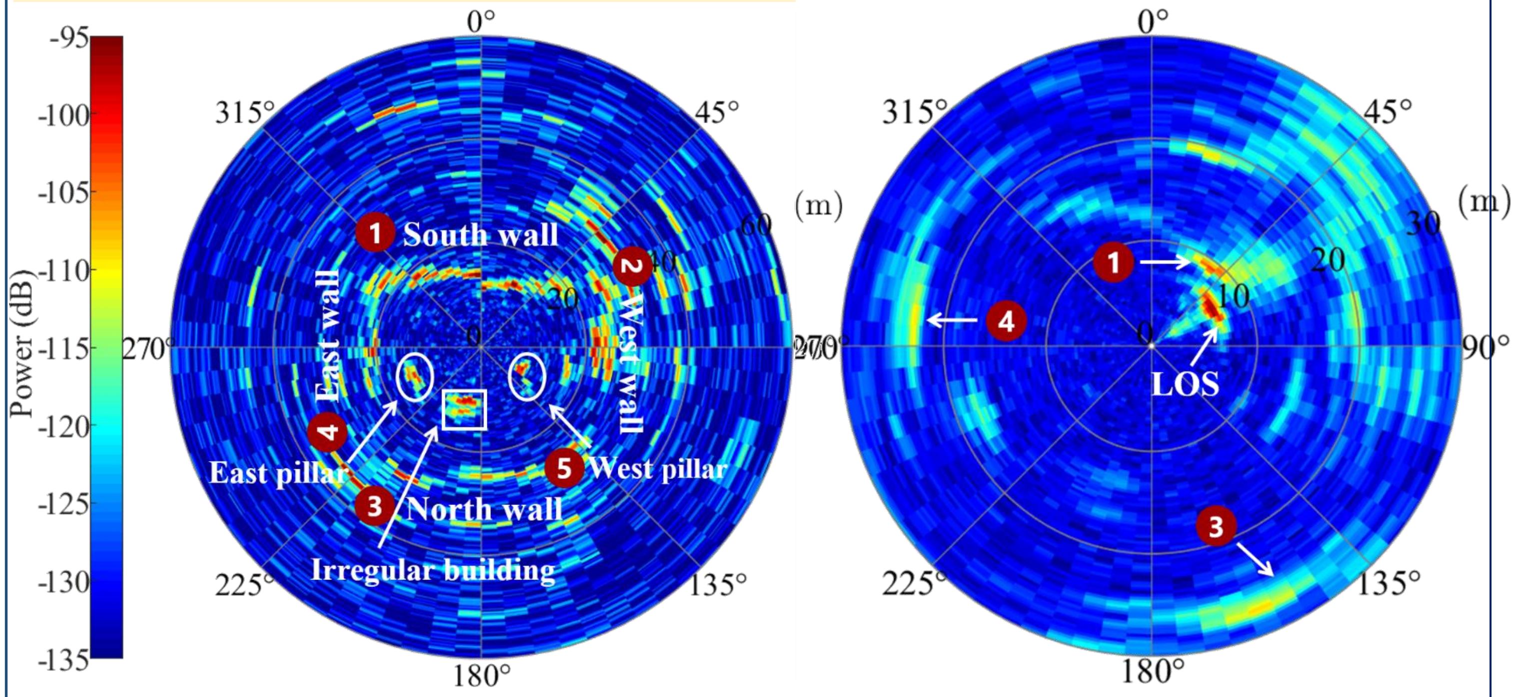

The sensing channel The communication channel

1 South wall, 3 north wall, and 4 east wall are defined as shared scatterers.

- *Y. Liu, J. Zhang, Y. Zhang, Z. Yuan, G. Liu , "A Shared Cluster-based Stochastic Channel Model for Joint Communication and Sensing Systems", arXiv preprint arXiv: 2211.06615, 2022.*

2.2 Small-scale fading modeling in JCAS channel

- A stochastic JCAS channel model based on shared clusters for capturing the sharing feature.

The illustration of JCAS channel model

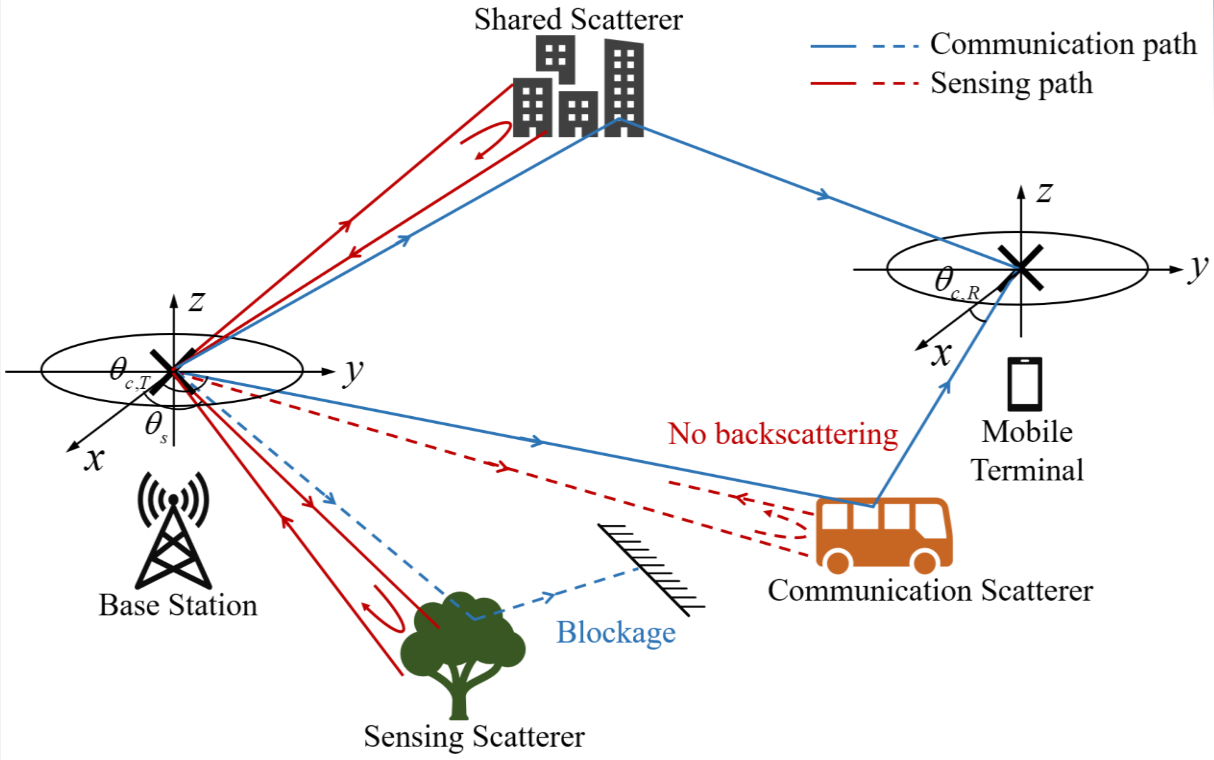

The JCAS channel model

CIR of communication:

Shared clusters

$$h_c(\theta_{c,R},\theta_{c,T},\tau_c) = \underbrace{\sum_{n_0=1}^{N_0}\sum_{m_0=1}^{M_0} a_{c,n_0,m_0}\delta(\theta_{c,R}-\theta_{c,n_0,m_0,R})\delta(\theta_{c,T}-\theta_{c,n_0,m_0,T})\delta(\tau_c-\tau_{c,n_0,m_0})}_{\text{Communication Shared Sub-Clusters}}$$
$$+\sum_{n_1=1}^{N_1}\sum_{m_1=1}^{M_1} a_{c,n_1,m_1}\delta(\theta_{c,R}-\theta_{c,n_1,m_1,R})\delta(\theta_{c,T}-\theta_{c,n_1,m_1,T})\delta(\tau_c-\tau_{c,n_1,m_1}),$$

Non-shared communication clusters

CIR of sensing:

$$h_s(\theta_{s,R},\theta_{s,T},\tau_s) = \underbrace{\sum_{n_0=1}^{N_0}\sum_{m_0=1}^{M_0} a_{s,n_0,m_0}\sigma_{n_0,m_0}\delta(\theta_{s,R}-\theta_{s,n_0,m_0,R})\delta(\theta_{s,T}-\theta_{s,n_0,m_0,T})\delta(\tau_s-\tau_{s,n_0,m_0})}_{\text{Sensing Shared Sub-Clusters}}$$
$$+\sum_{n_2=1}^{N_2}\sum_{m_2=1}^{M_2} a_{s,n_2,m_2}\sigma_{n_2,m_2}\delta(\theta_{s,R}-\theta_{s,n_2,m_2,R})\delta(\theta_{s,T}-\theta_{s,n_2,m_2,T})\delta(\tau_s-\tau_{s,n_2,m_2}).$$

Non-shared sensing clusters

- *Y. Liu, J. Zhang, Y. Zhang, Z. Yuan, G. Liu , "A Shared Cluster-based Stochastic Channel Model for Joint Communication and Sensing Systems", arXiv preprint arXiv: 2211.06615, 2022.*

2.2 Small-scale fading modeling in JCAS channel

- The sharing degree metric is derivated, and the practicality and controllability of the JCAS model are validated by simulations.

Sharing degree

$$\mathrm{SD}_s = \frac{P_s^{\mathrm{shared}}}{P_s^{\mathrm{total}}} = \frac{\left|\sum_{n_0}\sum_{m_0} a_{s}, n_0, m_0, \sigma_{n_0,m_0}\right|^2}{\left|\sum_{n_0}\sum_{m_0} a_{s}, n_0, m_0, \sigma_{n_0,m_0} + \sum_{n_2}\sum_{m_2} a_{s}, n_2, m_2, \sigma_{n_2,m_2}\right|^2}$$

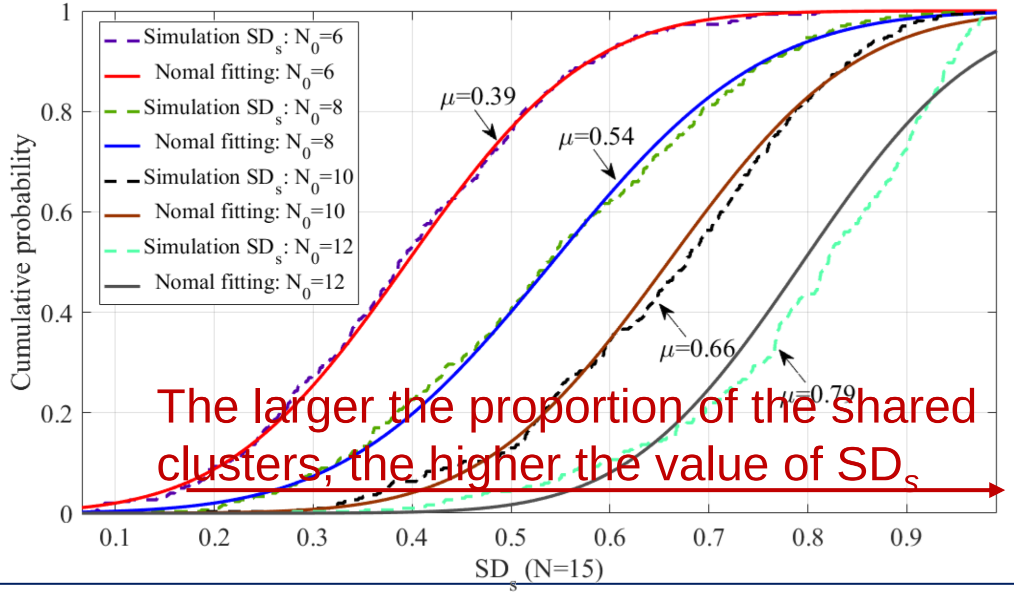

PDFs of cluster centroid AODs

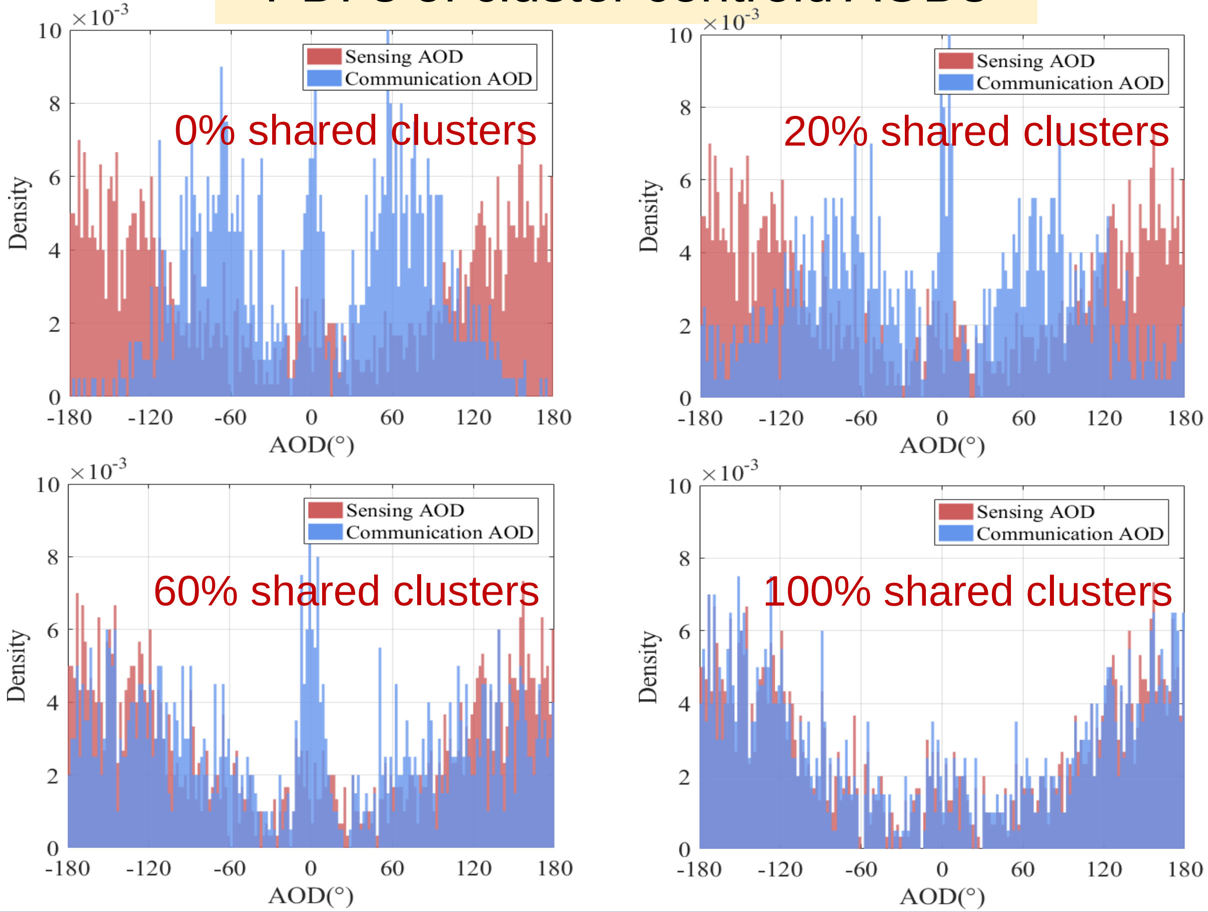

- *Y. Liu, J. Zhang, Y. Zhang, Z. Yuan, G. Liu , "A Shared Cluster-based Stochastic Channel Model for Joint Communication and Sensing Systems", arXiv preprint arXiv: 2211.06615, 2022.*

Outline

I. Trend and vision to 6G channel model

II. Our recent progress on 6G channel research

- Terahertz channel measurement and modeling
- Joint communication and sensing channel measurements and modeling
- Massive MIMO channel measurements and modeling
- Intelligent channel modeling and channel prediction

III. Work on 6G channel model standardization

3.1 Spatial non-stationary near-field channel modeling

- The near-field effect and spatial non-stationary characteristics are new challenges in massive MIMO channel modeling.

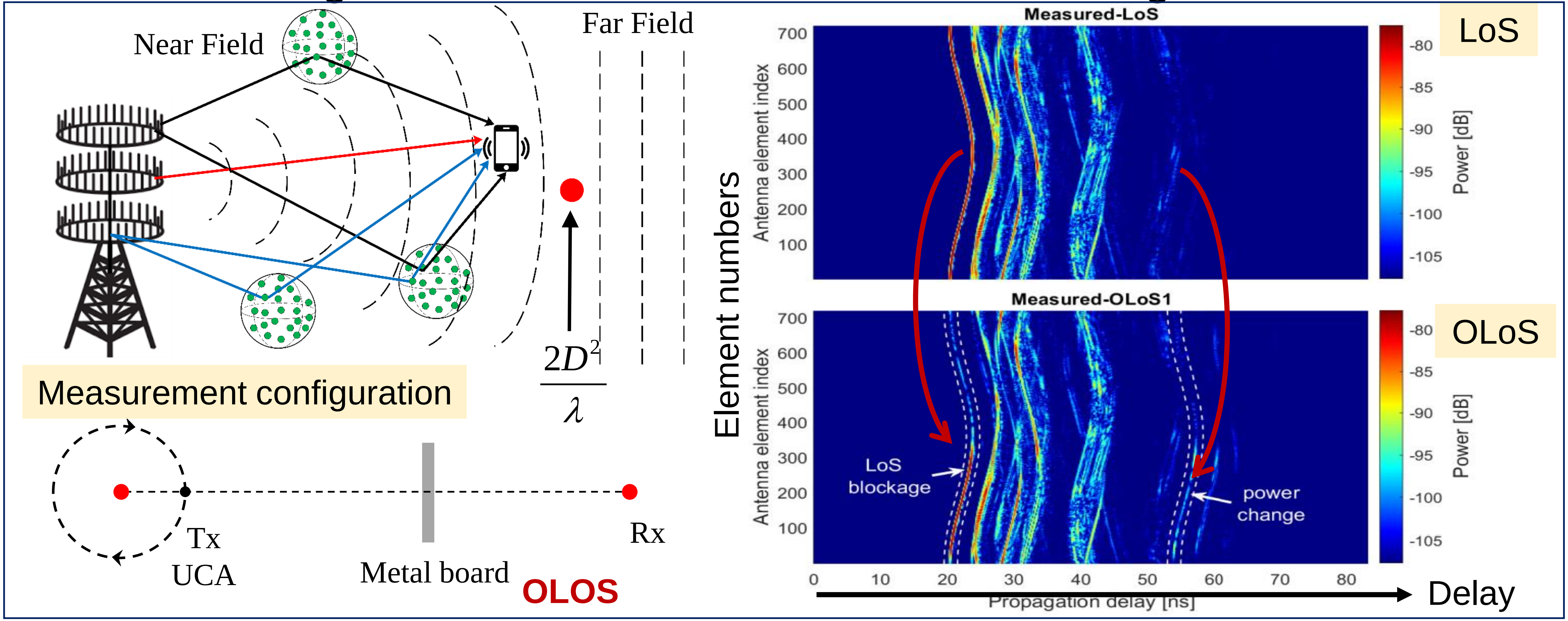

- *Z. Yuan, J. Zhang, Y. Ji, G. Pedersen, and W. Fan, "Spatial Non-stationary Near-field Channel Modeling and Validation for Massive MIMO Systems," IEEE Transactions on Antennas and Propagation, 2022.*

3.1 Spatial non-stationary near-field channel modeling

■ Spatial non-stationary (SnS) channel modeling framework.

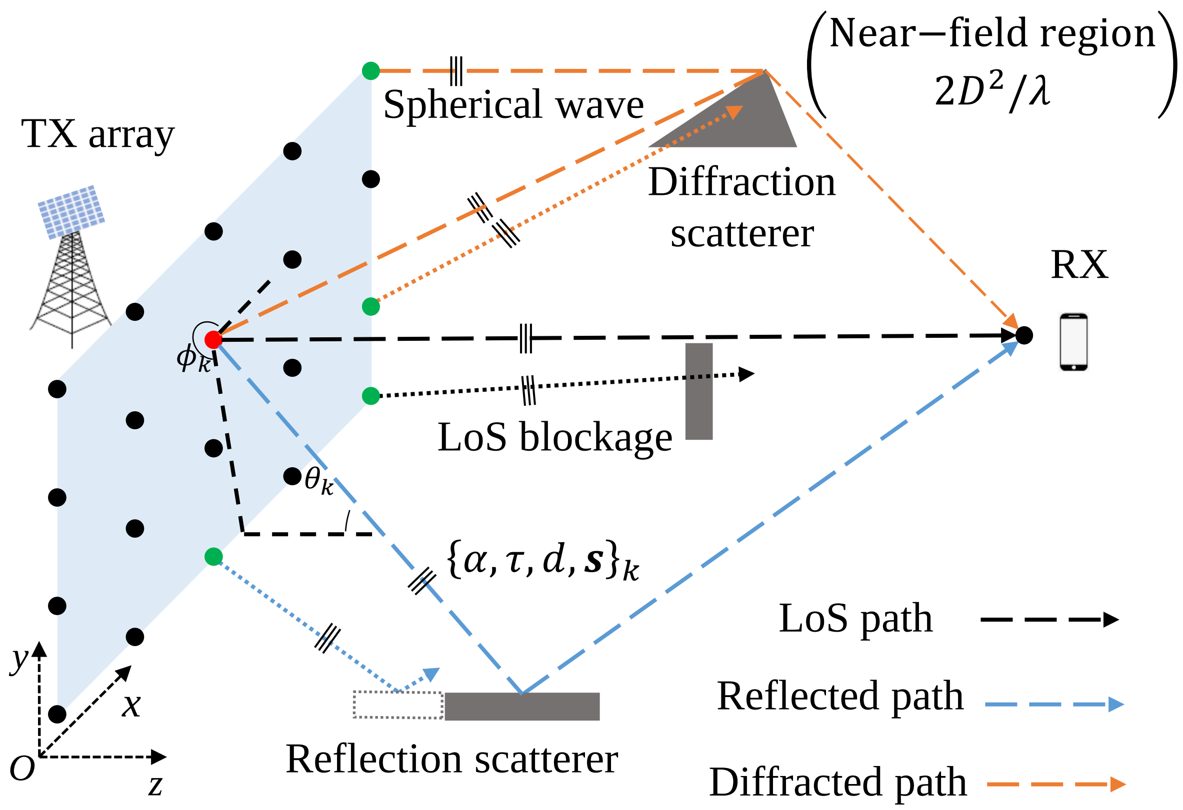

$$\boldsymbol{H} = \boldsymbol{S} \odot A(\theta, \phi, d) * H(\alpha, \tau, \theta, \phi)$$

SnS characteristic:

$$\boldsymbol{S}_{P\times k} = [\boldsymbol{s}_1, \boldsymbol{s}_2, \dots, \boldsymbol{s}_K] = [\{S_{pk}\}]$$

Near-field effect:

$$\boldsymbol{A}_{P\times K} = \left[\left\{ \frac{d_k}{d_{pk}} \exp(-j2\pi(d_{pk} - d_k)/c) \right\}_{p,k} \right]$$

$$\boldsymbol{H}(f) = [\alpha_1 \exp(-j2\pi f \tau_1), \dots, \alpha_K \exp(-j2\pi f \tau_K)]^T$$

- *Z. Yuan, J. Zhang, Y. Ji, G. Pedersen, and W. Fan, "Spatial Non-stationary Near-field Channel Modeling and Validation for Massive MIMO Systems," IEEE Transactions on Antennas and Propagation, 2022.*

3.1 Spatial non-stationary near-field channel modeling

- Spatial non-stationary (SnS) channel modeling validation.

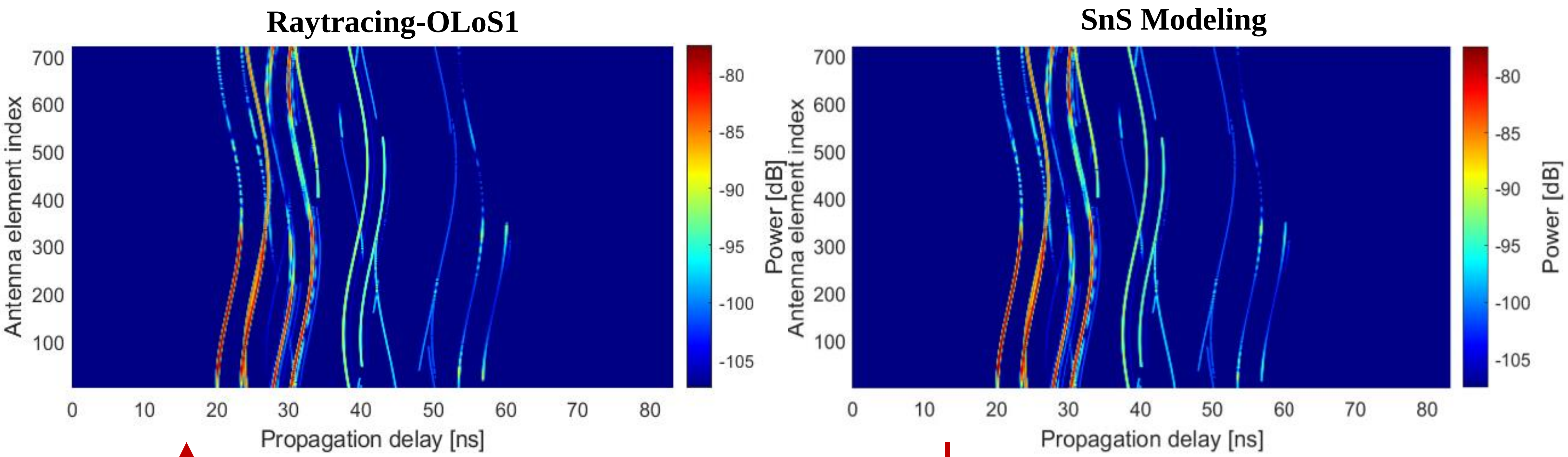

Accuracy ↑

Modeling settings	LoS	OLoS1	OLoS2
Stationary channel-$s_{m,k} = 1$	67.7%	41.2%	49.5%
SnS channel-$s_{m,k} \geqslant 0$	97.1%	96.2%	94.5%

Complexity ↓

Simulation with 720 antenna elements	Ray-tracing	SnS model
Time	12 hours	1 minute

- *Z. Yuan, J. Zhang, Y. Ji, G. Pedersen, and W. Fan, "Spatial Non-stationary Near-field Channel Modeling and Validation for Massive MIMO Systems, " IEEE Transactions on Antennas and Propagation, 2022.*

3.2 RIS-assisted channel modeling

- Compared with the traditional Tx-Rx channel, RIS cascade channel and RIS radiation pattern are required in RIS channel.

Tx-Rx channel model

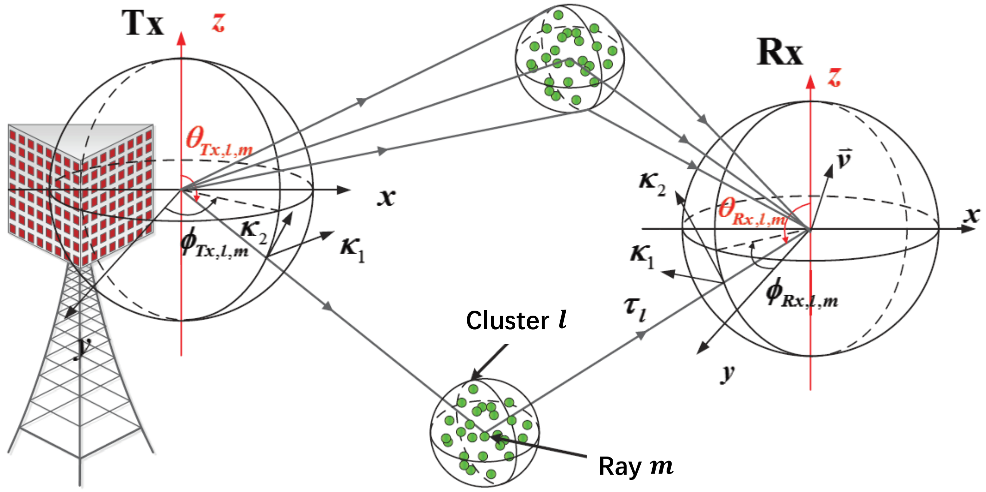

$$h_{u,s}(t,\tau)=\sum_{l,m}\mathbf{F}_{\mathrm{Rx}}{}^{T}\boldsymbol{\chi}_{l,m}\,\mathbf{F}_{\mathrm{Tx}}\,exp\left(j2\pi\lambda_0^{-1}\boldsymbol{r}_{\mathrm{Rx},l,m}^{T}\boldsymbol{d}_{\mathrm{Rx},u}\right)exp\left(j2\pi\lambda_0^{-1}\boldsymbol{r}_{\mathrm{Tx},l,m}^{T}\boldsymbol{d}_{\mathrm{Tx},s}\right)\times exp\left(j2\pi\lambda_0^{-1}\boldsymbol{v}_{l,m}t\right)\delta(\tau-\tau_{l,m})$$

Tx/Rx pattern: $\mathbf{F}_{\mathrm{Rx}}=\mathbf{F}_{\mathrm{Rx}}(\theta_{\mathrm{Rx},l,m},\phi_{\mathrm{Rx},l,m})$, $\mathbf{F}_{\mathrm{Tx}}=\mathbf{F}_{\mathrm{Tx}}(\theta_{\mathrm{Tx},l,m},\phi_{\mathrm{Tx},l,m})$

Cross polarization matrix:
$\boldsymbol{\chi}_{l,m}=\boldsymbol{\chi}_{l,m}(\theta_{\mathrm{Rx},l,m},\phi_{\mathrm{Rx},l,m},\theta_{\mathrm{Tx},l,m},\phi_{\mathrm{Tx},l,m})$

RIS channel model

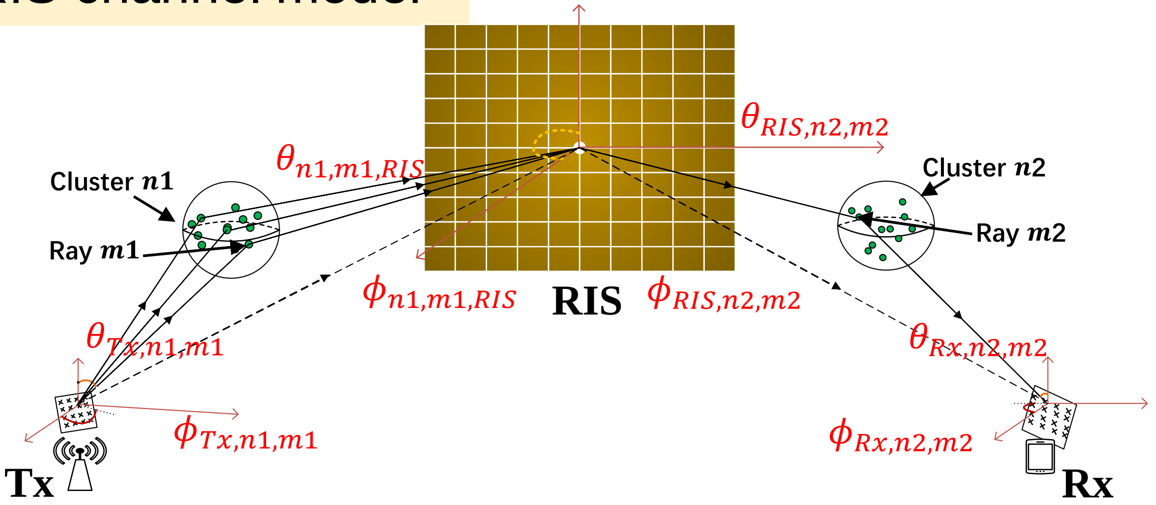

The cascade link — RIS radiation pattern

$$h_{u,s}(t,\tau)=\sum_{n1,m1}\sum_{n2,m2}\mathbf{F}_{\mathrm{Rx}}{}^{T}\boldsymbol{\chi}_{n2,m2}\,\mathbf{F}_{\mathrm{RIS}}\,\boldsymbol{\chi}_{n1,m1}\mathbf{F}_{\mathrm{Tx}}\,exp\left(j2\pi\lambda_0^{-1}\boldsymbol{r}_{\mathrm{Rx},n2,m2}^{T}\boldsymbol{d}_{\mathrm{Rx},u}\right)exp\left(j2\pi\lambda_0^{-1}\boldsymbol{r}_{\mathrm{Tx},n1,m1}^{T}\boldsymbol{d}_{\mathrm{Tx},s}\right)exp\left(j2\pi\lambda_0^{-1}\boldsymbol{v}_{n2,m2}t\right)\delta(\tau-\tau_{n1,m1}-\tau_{n2,m2})$$

$$\mathbf{F}_{\mathrm{RIS}}=\begin{bmatrix}F_{VV}(\theta_{n1,m1,RIS},\phi_{n1,m1,RIS},\theta_{RIS,n2,m2},\phi_{RIS,n2,m2}) & F_{VH}(\theta_{n1,m1,RIS},\phi_{n1,m1,RIS},\theta_{RIS,n2,m2},\phi_{RIS,n2,m2})\\ F_{HV}(\theta_{n1,m1,RIS},\phi_{n1,m1,RIS},\theta_{RIS,n2,m2},\phi_{RIS,n2,m2}) & F_{HH}(\theta_{n1,m1,RIS},\phi_{n1,m1,RIS},\theta_{RIS,n2,m2},\phi_{RIS,n2,m2})\end{bmatrix}$$

- *J. Zhang, Y. Zhang and L. Yu et al., "3-D MIMO: How Much Does It Meet Our Expectations Observed From Channel Measurements?," in IEEE Journal on Selected Areas in Communications, 2017.*

3.2 RIS-assisted channel modeling

- The electromagnetic response is related to the incident angle.

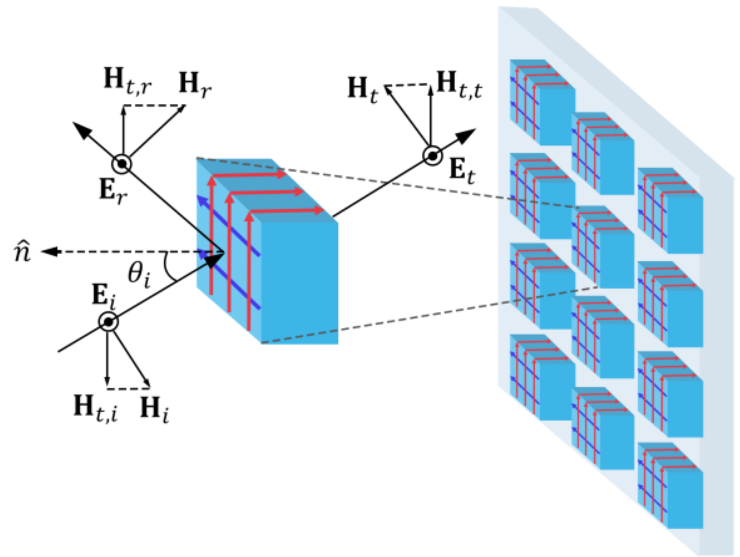

Equivalent impedance model

The deviation of incident angle ↑,
the deviation of reflection coefficient ↑

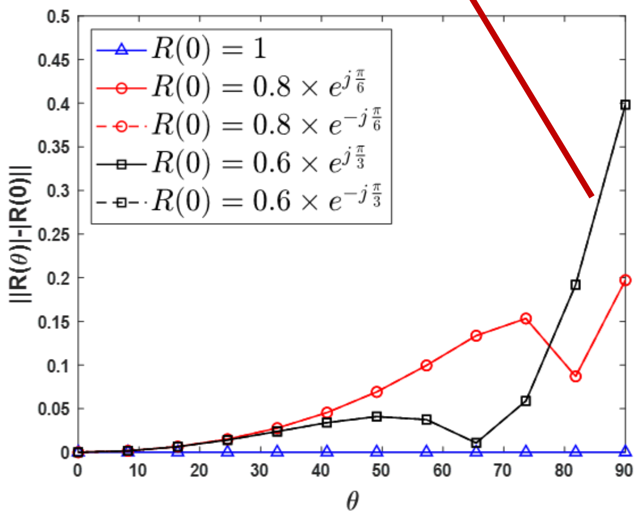

Amplitude deviation:

$||R(\theta)| - |R(0)||$

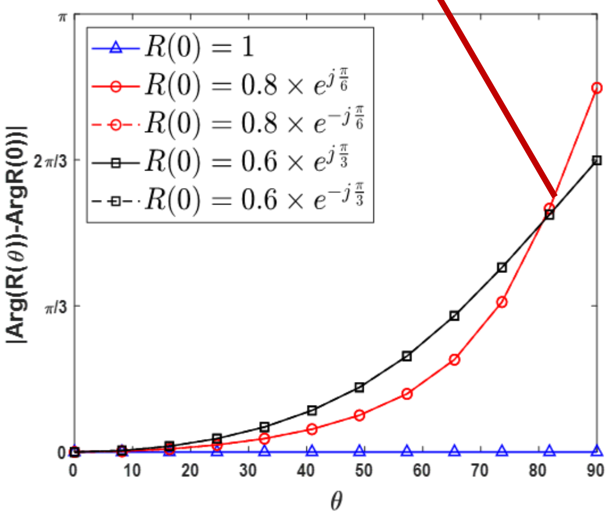

Phase deviation:

$|\mathrm{Arg}(R(\theta))\text{-}\mathrm{Arg}(R(0))|$

Reflection coefficient:

$$R(\theta) = \frac{-\eta_e}{2Z_e + \eta_e} + \frac{Z_m}{Z_m + 2\eta_e}$$

Vertical polarization: $\eta_e = \frac{\eta}{cos(\theta)}$ Parallel polarization: $\eta_e = \eta cos(\theta)$

- *J. Zhang, et al., "A deterministic channel modeling method for RIS-assisted communication in sub-THz frequencies,"17th European Conference on Antennas and Propagation (EuCAP), 2023, accepted.*

3.2 RIS-assisted channel modeling

Calculate RIS radiation pattern by physical optics (PO)

Calculate RIS scattering pattern

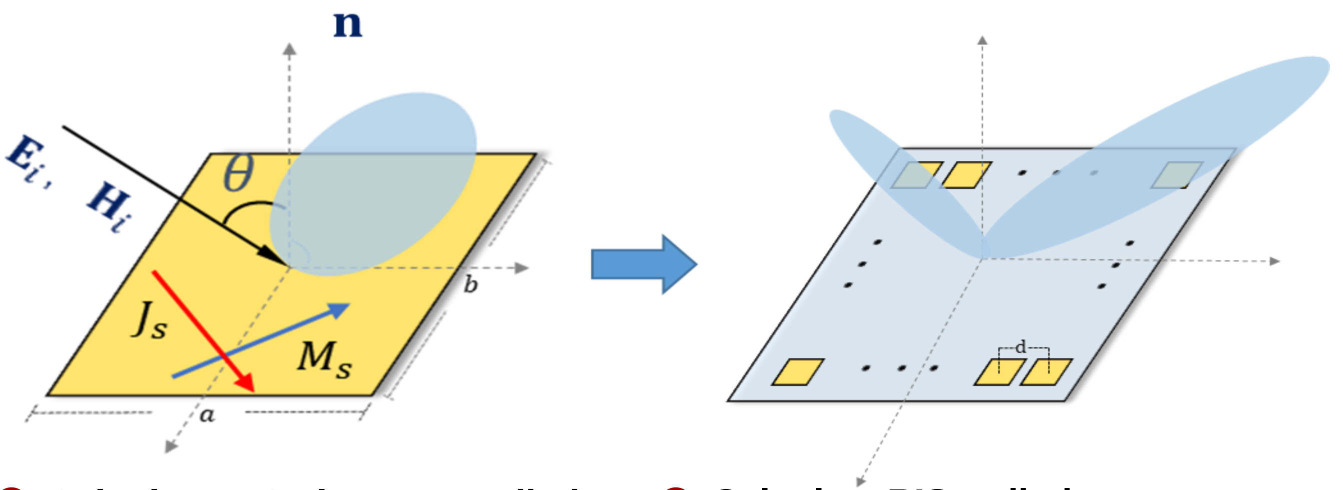

❶ **Calculate RIS elements radiation pattern by PO**

$$\mathbf{J}_s = \mathbf{n} \times (1 \mp R(\theta))\mathbf{H}_i$$
$$\mathbf{M}_s = -\mathbf{n} \times (1 \pm R(\theta))\mathbf{E}_i$$

The i-th RIS element radiation pattern:

$$f_{i,p1,p2} = f_{i,\mathbf{J}_s,\mathbf{M}_s,p1,p2}(\theta_{in}, \phi_{in}, \theta_{out}, \phi_{out})$$

❷ **Calculate RIS radiation pattern by superposition**

$$F_{p1,p2}(\theta_{in}, \phi_{in}, \theta_{out}, \phi_{out}) = \mathbf{w}_{in}{}^{T}\, diag(f_{1,p1,p2}, \dots, f_{N,p1,p2})\mathbf{w}_{out}$$

$\mathbf{w_{in}}^{\mathbf{T}}/\mathbf{w_{out}}$: **The array steering vector**

Simulation result

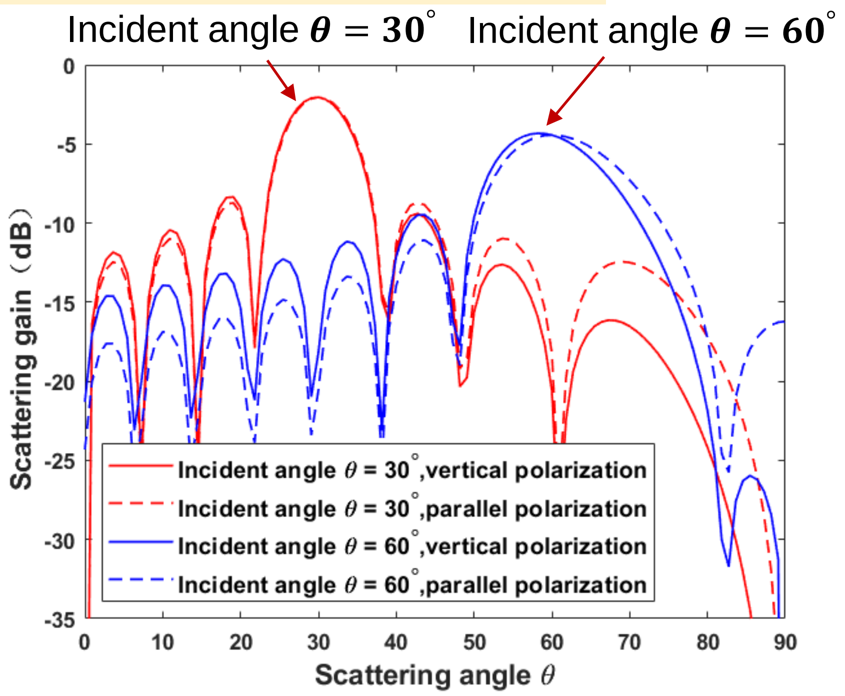

The incident angle and polarization are the factors affecting the RIS radiation pattern

- J. Zhang, Z. Zhou and Y. Zhang et al., *"A deterministic channel modeling method for RIS-assisted communication in sub-THz frequencies," 2023 17th European Conference on Antennas and Propagation (EuCAP), 2023, accepted.*

3.2 RIS-assisted channel modeling

- RIS cascade channel is generated, and delete low power clusters to reduce the complexity.

RIS cascade channel model

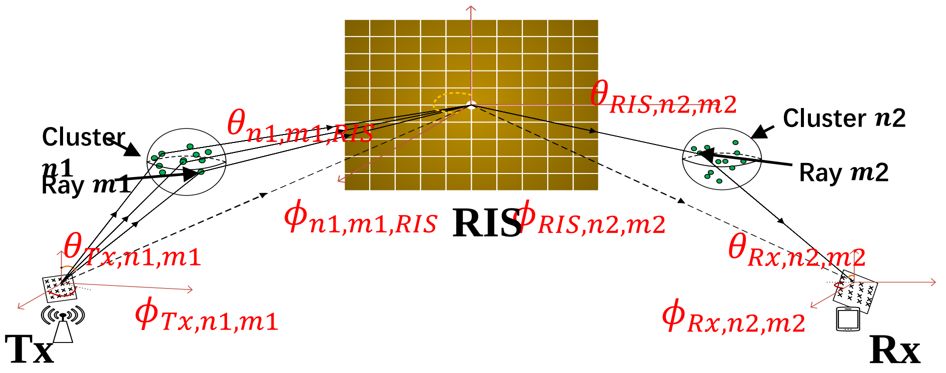

❶ **Generate the LSP and SSP of sub-channels:**

Tx-RIS: $\tau_{n1,m1}, P_{n1,m1}, \phi_{n1,m1,RIS}, \theta_{RIS,n1,m1}, \phi_{Tx,n1,m1}, \theta_{Tx,n1,m1}$

RIS-Rx: $\tau_{n2,m2}, P_{n2,m2}, \phi_{RIS,n2,m2}, \theta_{RIS,n2,m2}, \phi_{Rx,n1,m1}, \theta_{Rx,n1,m1}$

❷ **Calculate RIS radiation pattern:**

$$\mathbf{F}_{\mathrm{RIS}} = \mathbf{F}(\theta_{n1,m1,RIS}, \phi_{n1,m1,RIS}, \theta_{RIS,n2,m2}, \phi_{RIS,n2,m2})$$

❸ **Calculate CIR of RIS cascade channel:**

$$\boldsymbol{h}_{u,s}(\boldsymbol{t},\boldsymbol{\tau}) = \sum_{c,s}\sum_{m,n}\sqrt{P_{\mathrm{n1,m1}}P_{\mathrm{n2,m2}}}\mathbf{F}_{\mathrm{Rx}}{}^{T}\boldsymbol{\chi}_{n2,m2}\mathbf{F}_{\mathrm{RIS}}\boldsymbol{\chi}_{n1,m1}\mathbf{F}_{\mathrm{Tx}}e^{\left(\frac{j2\pi\left(\mathbf{r}_{Rx,n2,m2}^{T}\cdot\mathbf{d}_{Rx,u}+\mathbf{r}_{Tx,n1,m1}^{T}\cdot\mathbf{d}_{Tx,s}\right)}{\lambda}\right)} \times \delta(\tau-(\tau_{n1,m1}+\tau_{n2,m2}))$$

Cluster deletion

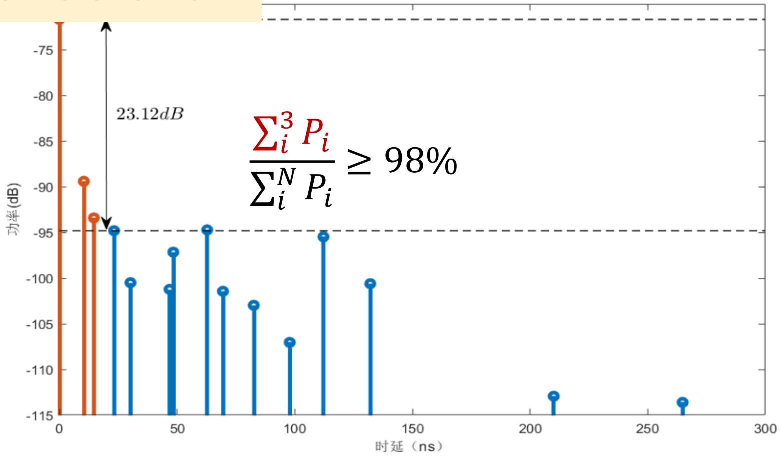

❶ **Delete clusters base on RIS pattern**

$$N_{cliped} = \sum_{n1}^{N} I\left(f_{i,p1,p2} \geq f_{th}\right), I(A) = \begin{cases} 1, A \text{ is true} \\ 0, \text{A is false.} \end{cases}$$

❷ **Delete clusters base on power ratio**

$$[P_1, P_2, \dots, P_N] = sort(\mathbf{P})$$

$$N_{cliped} = \min N_c, st. \frac{\sum_i^{N_c} P_i}{\sum_i^N P_i} \geq c\%$$

- *H. Gong, J. Zhang, Y. Zhang, et al., "How to Extend 3D GBSM Model to RIS Cascade Channel with Non-ideal Phase Modulation?," arXiv preprint arXiv:2302.07501, 2023.*

3.2 RIS-assisted channel modeling

- Modification of RIS channel modeling to standard flow.

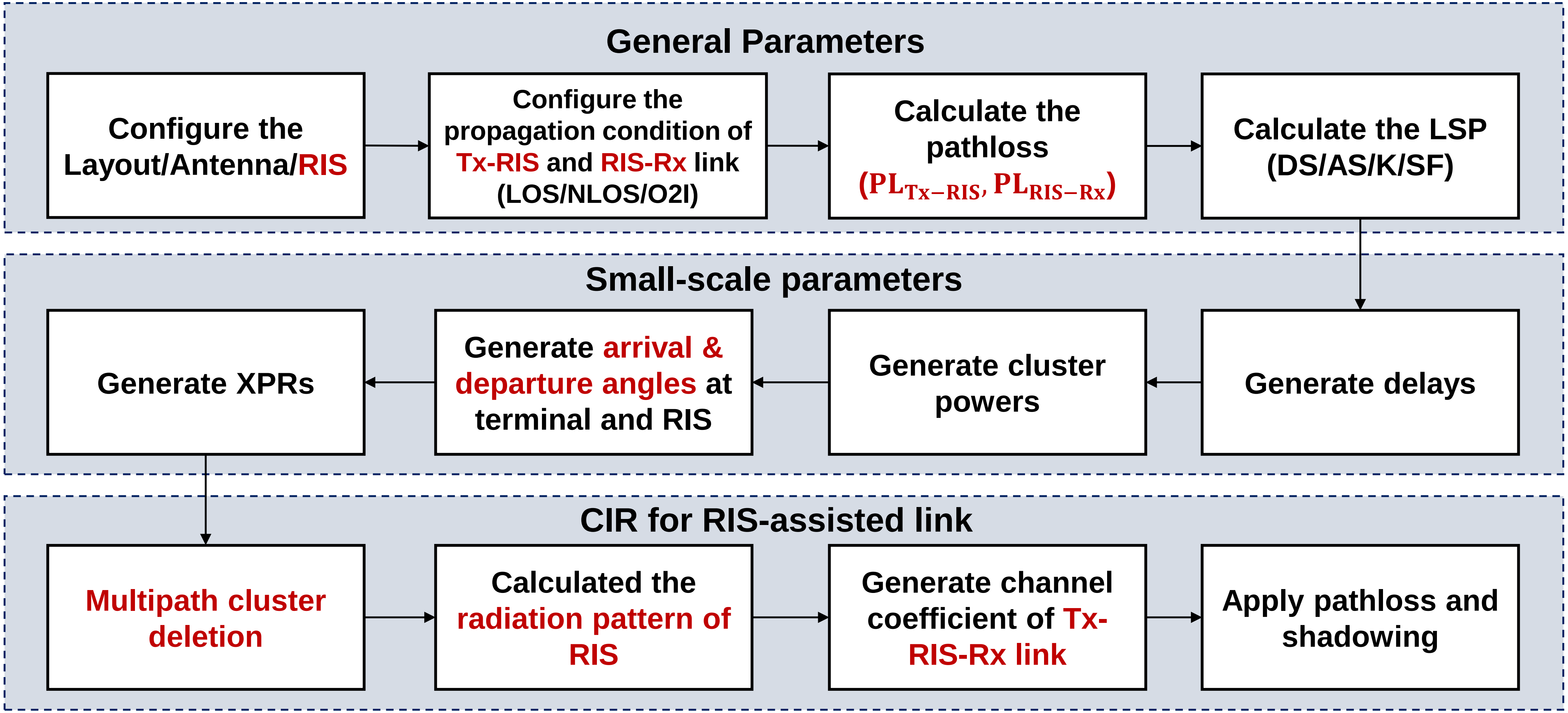

- *H. Gong, J. Zhang, Y. Zhang, et al., "How to Extend 3D GBSM Model to RIS Cascade Channel with Non-ideal Phase Modulation?," arXiv preprint arXiv:2302.07501, 2023.*

Outline

I. Trend and vision to 6G channel model

II. Our recent progress on 6G channel research

- Terahertz channel measurement and modeling
- Joint communication and sensing channel measurements and modeling
- Massive MIMO channel measurements and modeling
- Intelligent channel modeling and channel prediction

III. Work on 6G channel model standardization

4.1 Intelligent modeling

Mainstream channel modeling research

Category	**Deterministic Model**	**Stochastic Model**
Prerequisite	Environmental information	Measurement data
Clusters & rays generation	Environment-based & Deterministic	Random & Statistical
Advantages	High accuracy	Low complexity & generality
Disadvantages	High complexity	Low accuracy for practical environments
Modeling Procedure	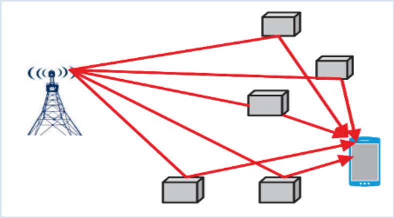	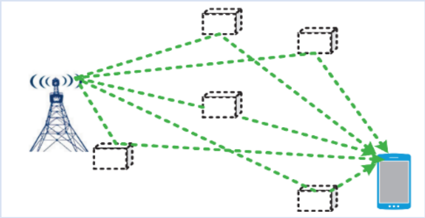

- *J. Zhang, "The interdisciplinary research of big data and wireless channel: A cluster-nuclei based channel model," China Communs, 2016. (First Best Paper Award)*

4.1 Intelligent modeling

A Cluster-nuclei based channel model

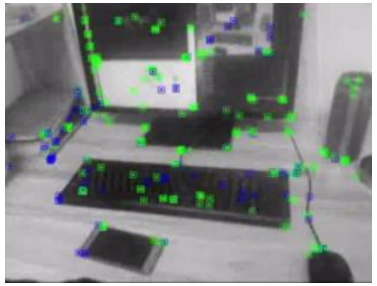

Machine learning,
Pattern recognition,
Image processing

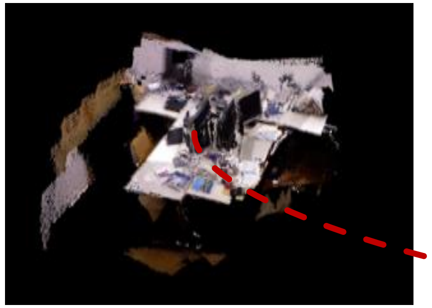

Environmental scatters + **Stochastic clusters**

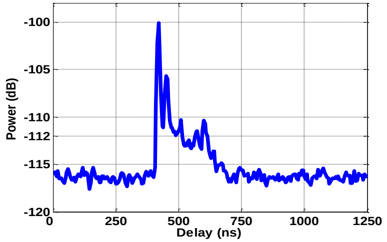

Estimation,
Signal processing,
Statistics,
Clustering

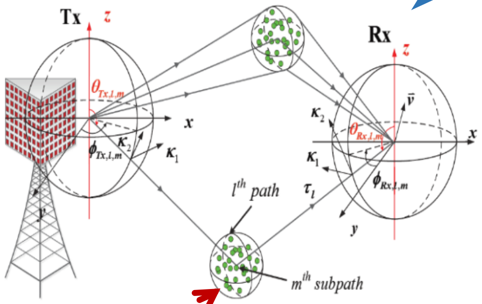

Matching of scatters and clusters

Cluster-nuclei

variation rules of channel characteristics by data mining

Channel modeling theory

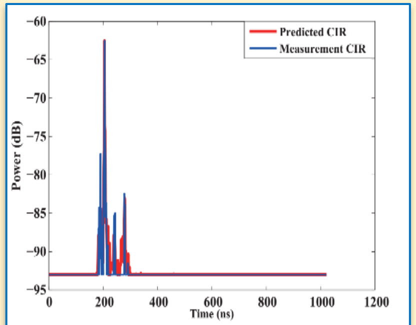

Fig. 11: CIR prediction by Elman neural network

- *J. Zhang, "The interdisciplinary research of big data and wireless channel: A cluster-nuclei based channel model," China Communs, 2016. (First Best Paper Award)*

4.1 Intelligent modeling

An implementation framework of cluster-nuclei based channel model

Propagation environment

Radar SLAM

Environment reconstruction

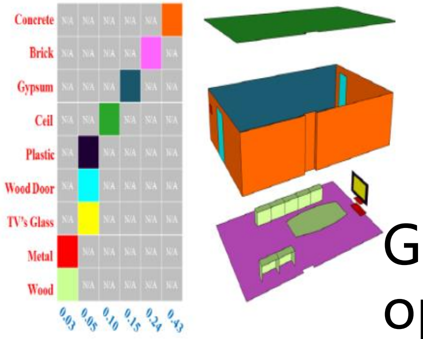

Geometric optics

Cluster-nuclei mapping

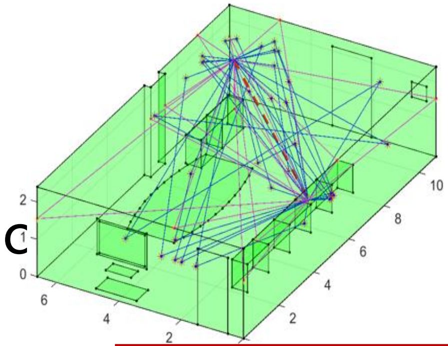

Friis & Fresnel equations

Cluster-nuclei calculation

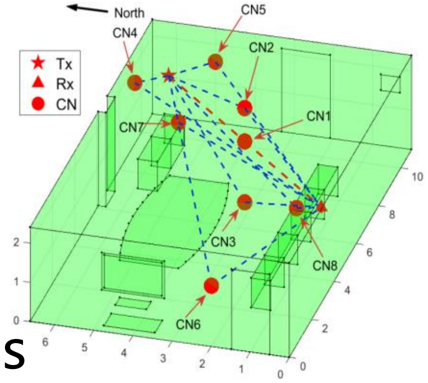

$$h_{u,s}(t,\tau) = \sum_{n=1}^{N} f(CN_n, \pi_n) = \sum_{n=1}^{N}\sum_{m=1}^{M} g_{n,m} \times exp(j2\pi t v_{n,m})\delta(\tau - \tau_{n,m})$$

Cluster-Nuclei

Accuracy is increased by 11.5%

	lgASA	lgASD	lgDS
Target channel	1.3146	1.5937	0.7158
Cluster-nuclei model	1.3161	1.6147	0.7233
Stochastic model	1.2161	1.5047	0.3982

- *L. Yu, Y. Zhang, J. Zhang, Implementation framework and validation of cluster-nuclei based channel model using environmental mapping for 6G communication systems, China Communs, 2022.*

4.2 Path loss prediction based on environmental features

- A environment features-based model (EFBM) for the large-scale prediction is proposed by mining the effective environmental attributes

Propagation-related environmental features extraction

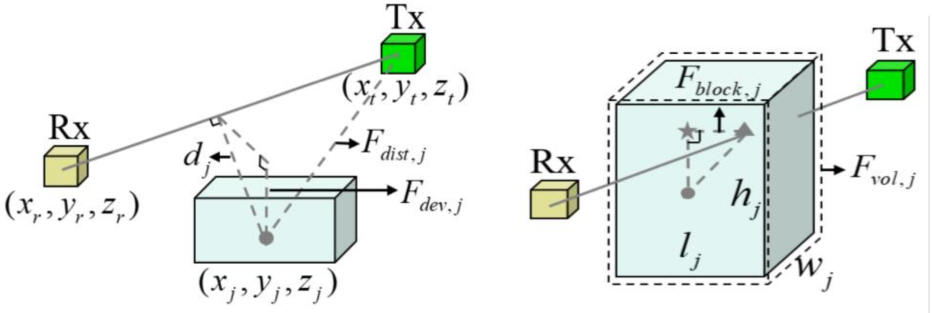

Distance feature

Volume feature

$$\{F_{dist,j}, F_{dev,j}, F_{vol,j}, F_{block,j}\}$$

Deviation feature

Blockage feature

RMSE drops at 0.89 dB@28 GHz

RMSE drops at 0.33 dB@6 GHz

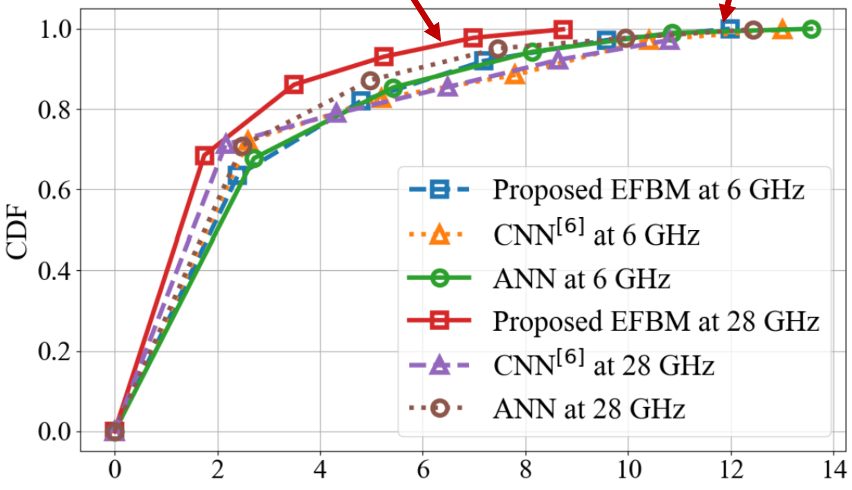

CDF figures of prediction by different methods (dB)

- *Y. Sun, J. Zhang, Y. Zhang et al., "Environment Features-Based Model for Path Loss Prediction," IEEE Wireless Communications Letters, 2022.*

4.3 Environment reconstruction and feature extraction

- Oriented to task, propagation environment semantics (PES) is defined and extraction by proposed environment-channel-task architecture.

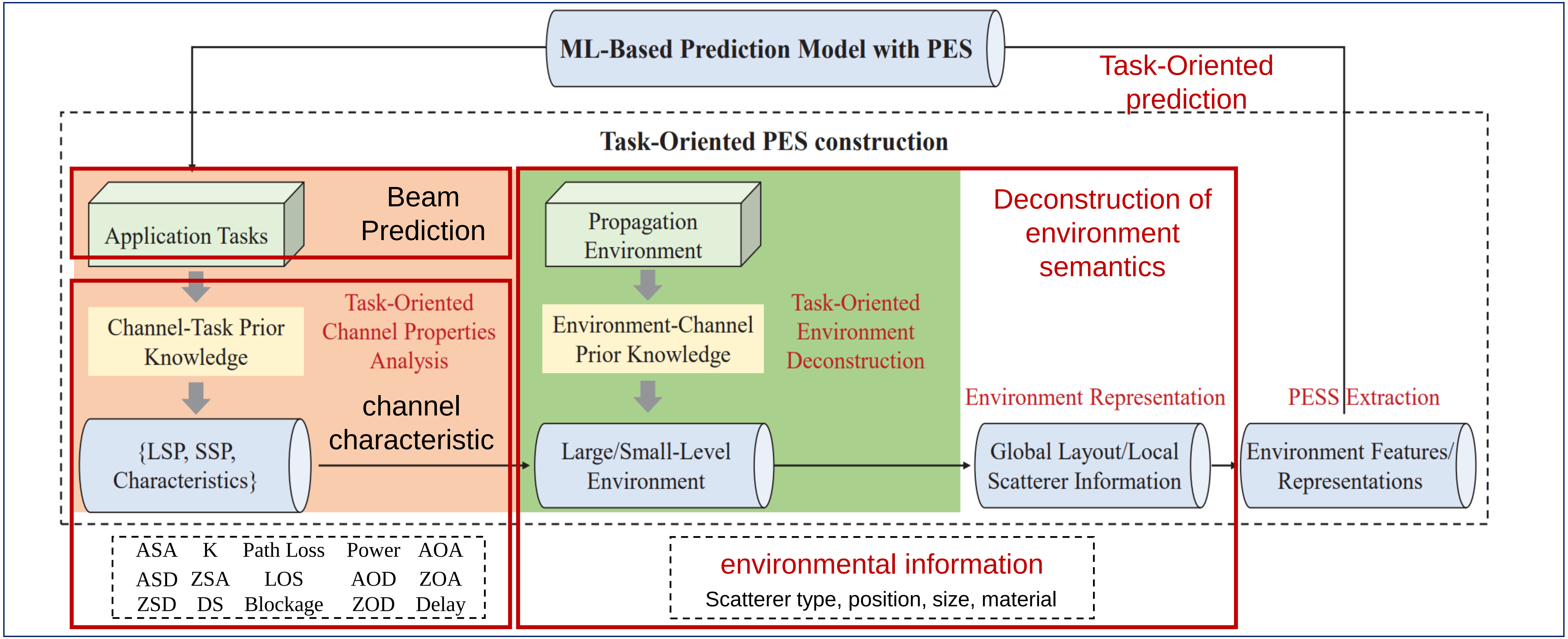

- *Y. Sun, J. Zhang, et al., "How to Define the Propagation Environment Semantics and Its Application in Scatterer-Based Beam Prediction," IEEE Wireless Communications Letters, 2023, early access.*

4.3 Environment reconstruction and feature extraction

- Beam prediction method is proposed based on the PES and channel mapping principle, which can improve precision and reduce complexity.

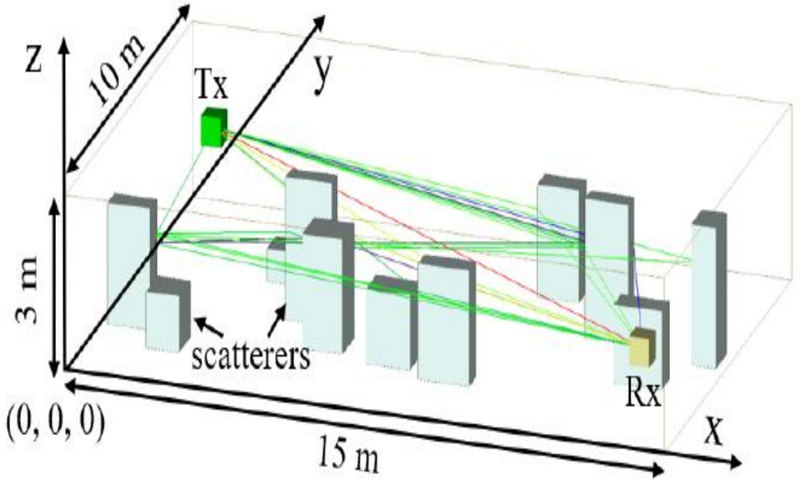

A simulated sample with a random scatterer layout.

Compared with the image-based beam indices, the accuracy is improved by more than 6%

Action	Configuration	Precision
Proposed Channel Quality Evaluation	\	0.92
Proposed Target Scatterer Detection	\	0.90
Beam Indices Prediction in [4]	Top-1	0.51
	Top-2	0.72
	Top-3	0.84

87% of the prediction time is saved

Action	Testing time (ms)
Proposed Channel Quality Evaluation	4.7
Proposed Target Scatterer Detection	0.33
Beam Indices Prediction in [4]	41

- *Y. Sun, J. Zhang, et al., "How to Define the Propagation Environment Semantics and Its Application in Scatterer-Based Beam Prediction," IEEE Wireless Communications Letters, 2023, early access.*

4.3 Environment reconstruction and feature extraction

- A sensing-prediction-decision architecture is used to transform the paradigm for offline modeling-online prediction.

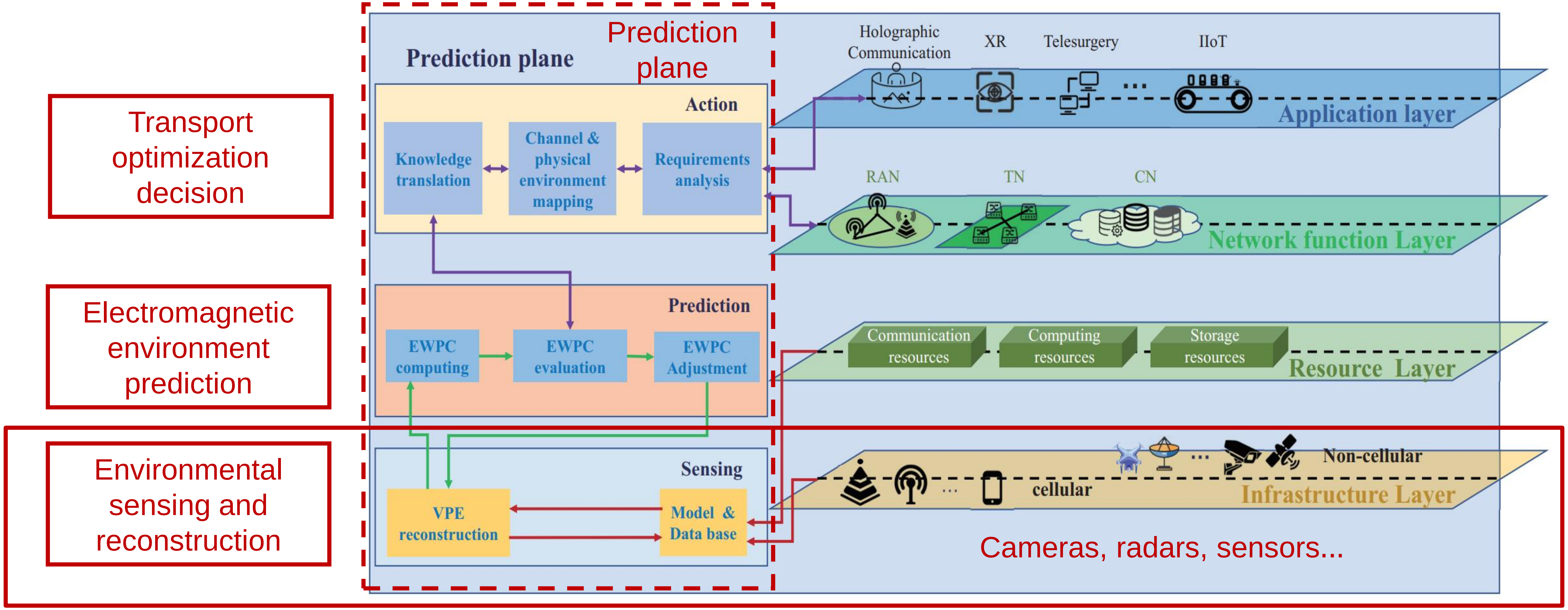

Cover article of China Communications 2022 issue 6

- *G. Nie, J. Zhang, et al., "A Predictive 6G Network with Environment Sensing Enhancement: From Radio Wave Propagation Perspective" China Communications, 2022. (COVER ARTICLE)*

4.4 Diffraction characteristics based blockage prediction

- An interesting phenomenon is found that the received power fluctuates with an increasing amplitude before the blockage occurrence.

Human body blockage at 28GHz

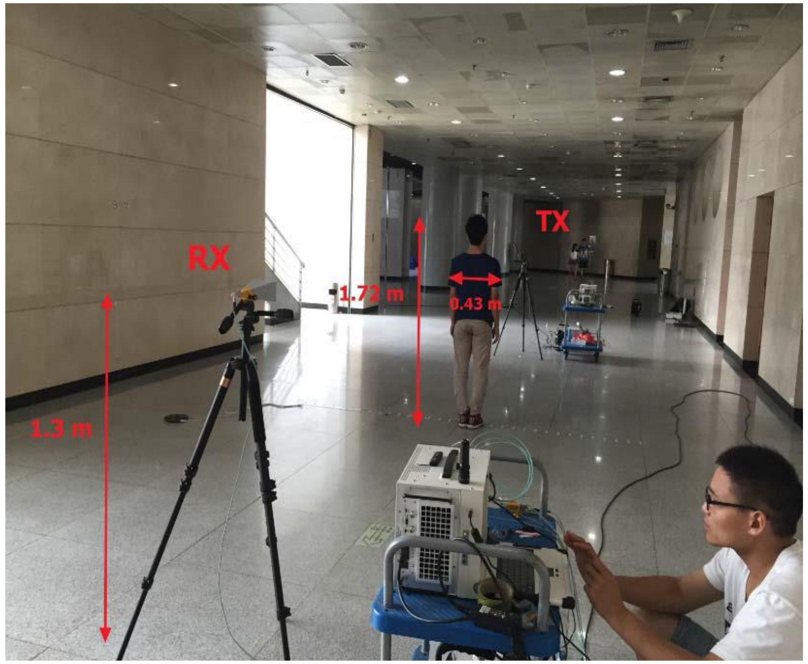

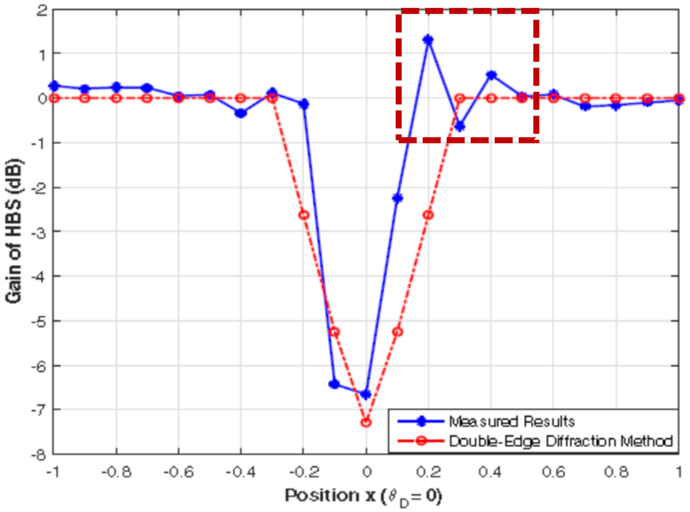

Double edge model

$$G_l = \frac{1+j}{2}\left\{\left(\frac{1}{2} - C(v)\right) - j\left(\frac{1}{2} - S(v)\right)\right\}$$

Pedestrian blockage at 73GHz

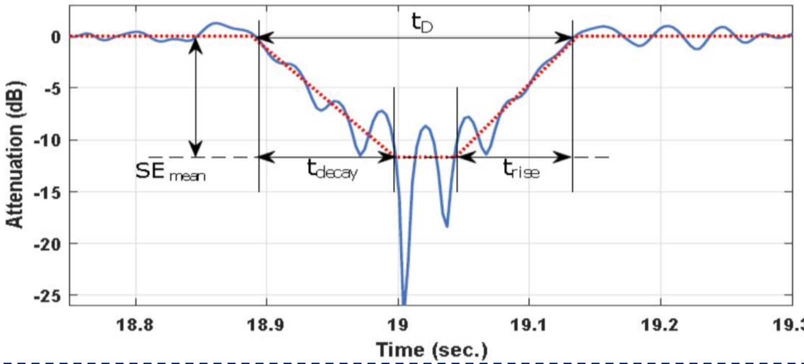

- X. Chen, L. Tian, P. Tang and J. Zhang, "Modelling of Human Body Shadowing Based on 28 GHz Indoor Measurement Results," 2016 IEEE 84th Vehicular Technology Conference (VTC-Fall), 2016.
- G. R. MacCartney, T. S. Rappaport and S. Rangan, "Rapid Fading Due to Human Blockage in Pedestrian Crowds at 5G Millimeter-Wave Frequencies," GLOBECOM 2017 - 2017 IEEE Global Communications Conference, 2017.

4.4 Diffraction characteristics based blockage prediction

- Optical principles are introduced into wireless communication analysis

Huygens' principle → **Fresnel-Kirchhoff formula** → **Diffraction fringe characteristics**

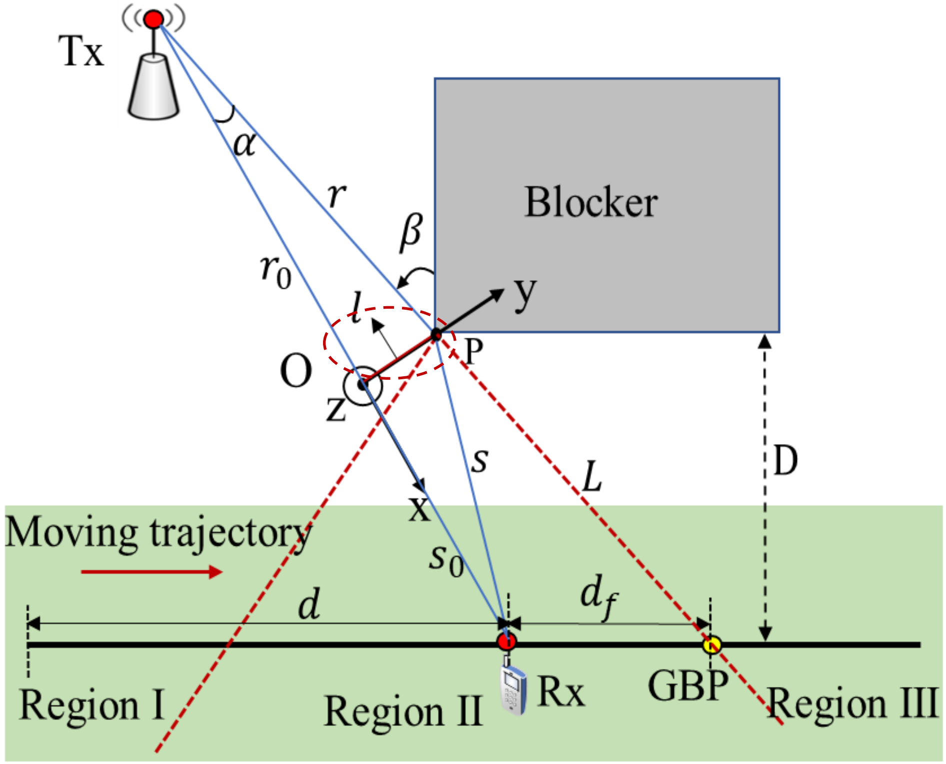

Electric field strength: $$E_{rx} = -\frac{E_0}{\lambda}\frac{i}{r_0 s_0}\iint_S e^{ik(r+s)}dS$$

Sum of secondary sources

$$r, s \rightarrow r_0, s_0$$

$$E_{rx} = B\left(C_{int} + iS_{int}\right) \qquad B = -\frac{E_0 i}{\lambda}\frac{e^{ik(r_0+s_0)}}{r_0 s_0}$$

Cosine component: $$C_{int} = \iint_S \cos\left[kf(y,z)\right]dydz$$

Sine component: $$S_{int} = \iint_S \sin\left[kf(y,z)\right]dydz$$

$$f(y,z) = \frac{1}{2}\left(\frac{1}{r_0} + \frac{1}{s_0}\right)(y^2 + z^2)$$

- L. Yu, J. Zhang, Y. Zhang, et al., "Long-Range Blockage Prediction Based on Diffraction Fringe Characteristics for mmWave Communications," IEEE Communications Letters, 2022.

4.4 Diffraction characteristics based blockage prediction

- By introducing Fresnel integral, the frequency dependent diffraction fringe is derived, which can serve as a blockage indicator.

Integration variables transformation

$$C_{int} = b\int_{-\infty}^{w} du \int_{-\infty}^{+\infty} dv \cos\left[\frac{\pi}{2}\left(u^2+v^2\right)\right] \qquad \frac{\pi}{\lambda}\left(\frac{1}{r_0}+\frac{1}{s_0}\right)y^2 = \frac{\pi}{2}u^2$$

$$S_{int} = b\int_{-\infty}^{w} du \int_{-\infty}^{+\infty} dv \sin\left[\frac{\pi}{2}\left(u^2+v^2\right)\right] \qquad \frac{\pi}{\lambda}\left(\frac{1}{r_0}+\frac{1}{s_0}\right)z^2 = \frac{\pi}{2}v^2$$

Introduce Fresnel integral

$$\mathrm{C}(w)=\int_{0}^{w}\cos\left(\frac{\pi}{2}\tau^2\right)d\tau \qquad \mathrm{S}(w)=\int_{0}^{w}\sin\left(\frac{\pi}{2}\tau^2\right)d\tau$$

Received power at Rx

$$P_{rx} = \frac{1}{2}\left\{\left[\frac{1}{2}+\mathrm{C}(w)\right]^2+\left[\frac{1}{2}+\mathrm{S}(w)\right]^2\right\}P_{rx0}$$

$$P_{rx0} = \frac{|E_0|^2}{(r_0+s_0)^2} \qquad w = \sqrt{\frac{2f\cdot d_f^2}{c}\,\frac{r_0\cos^2\beta}{D(r_0\cos\beta+D)}}$$

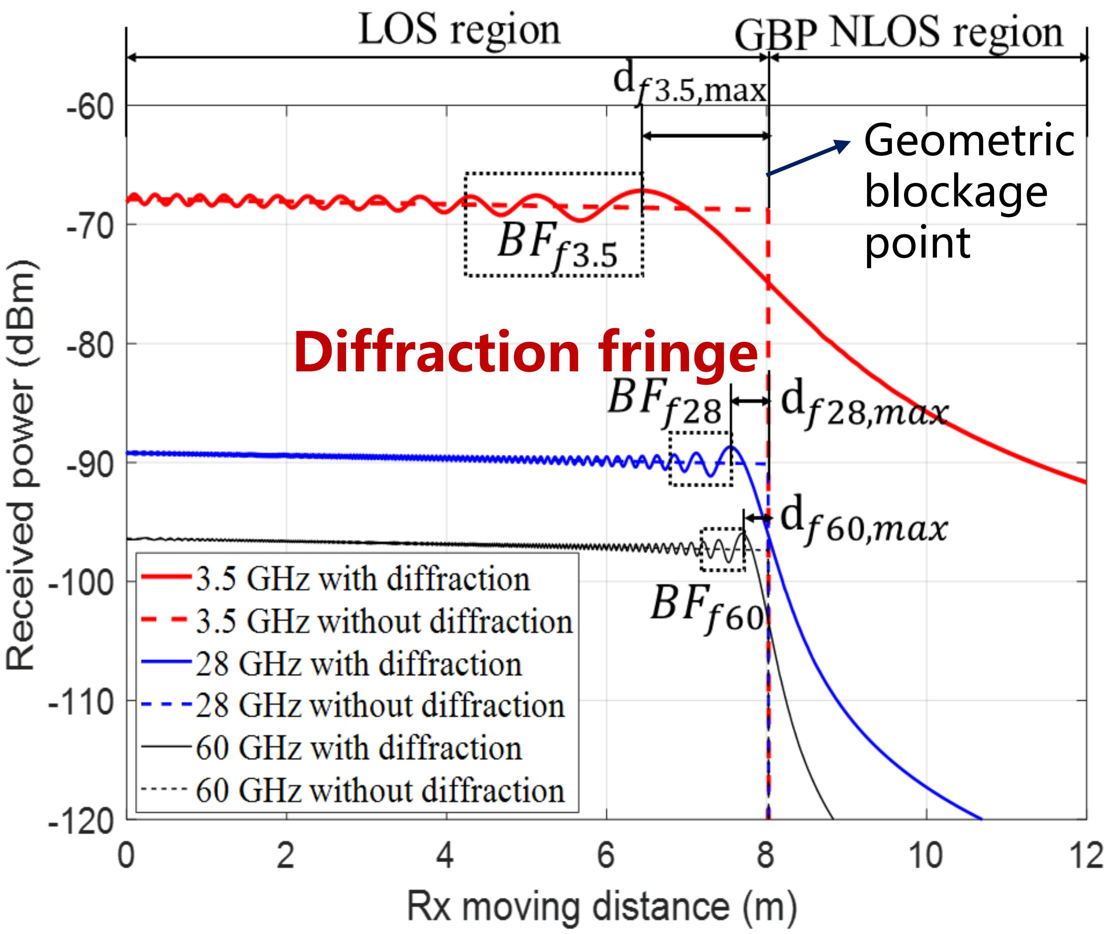

- L. Yu, J. Zhang, Y. Zhang, et al., "Long-Range Blockage Prediction Based on Diffraction Fringe Characteristics for mmWave Communications," IEEE Communications Letters, 2022.

4.4 Diffraction characteristics based blockage prediction

- Inspired by diffraction fringe, a BF based prediction scheme is proposed to detect an upcoming blockage using sliding correlation.

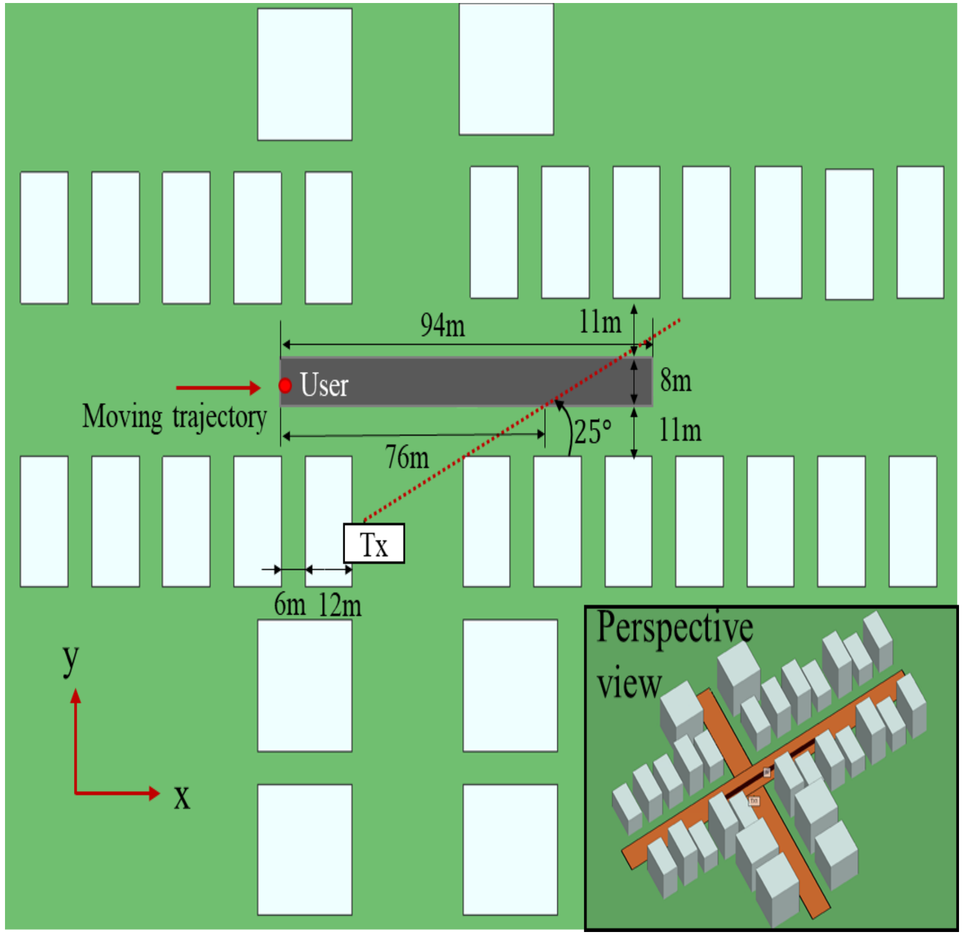

Sliding Correlation: $\gamma(d) = \frac{\sum_i (\eta_{f,i}^{BF} - \bar{\eta}_f^{BF})(\tilde{\eta}_{rx,i}(d) - \bar{\eta}_{rx}(d))}{\sqrt{\sum_i (\eta_{f,i}^{BF} - \bar{\eta}_f^{BF})^2}\sqrt{\sum_i (\tilde{\eta}_{rx,i}(d) - \bar{\eta}_{rx}(d))^2}}$

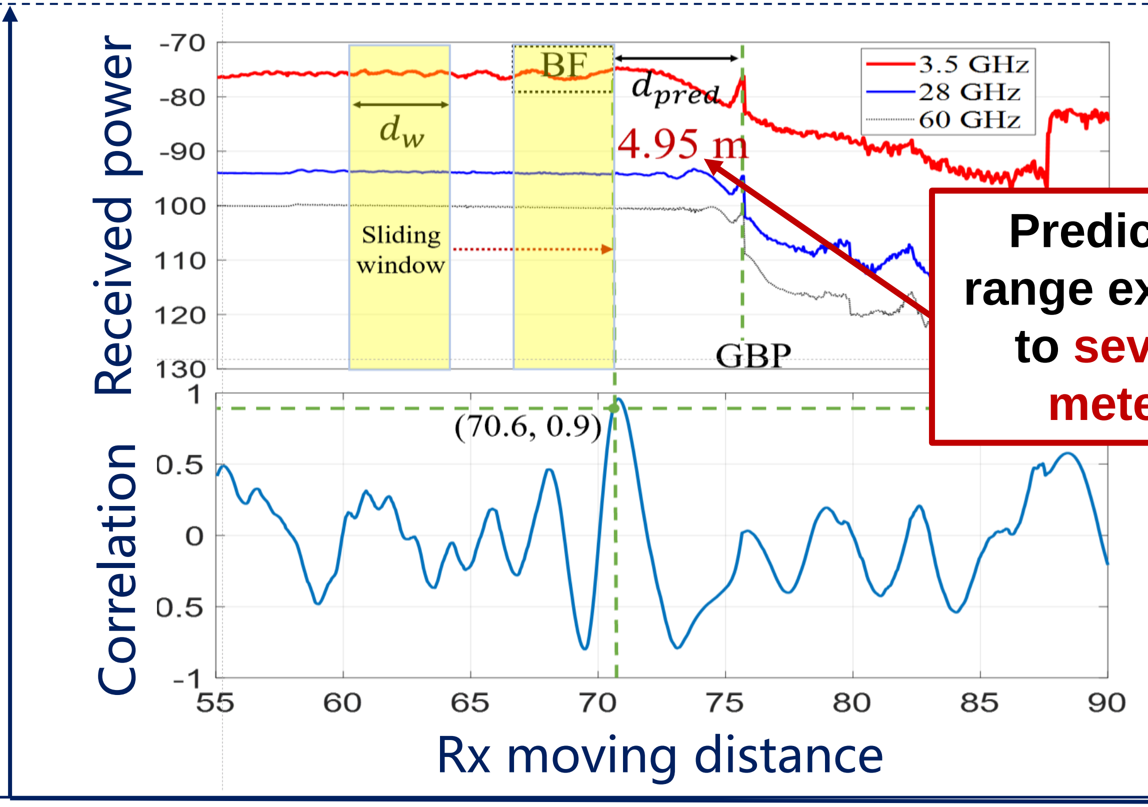

Prediction range extends to several meters

- L. Yu, J. Zhang, Y. Zhang, et al., "Long-Range Blockage Prediction Based on Diffraction Fringe Characteristics for mmWave Communications," IEEE Communications Letters, 2022.

4.5 Platform 1: predictive 6G network via enhanced sensing

- In Dec. 2022, PREDICT-Plat was released capable of predicting and reconstructing wireless environments with sensing enhancement.

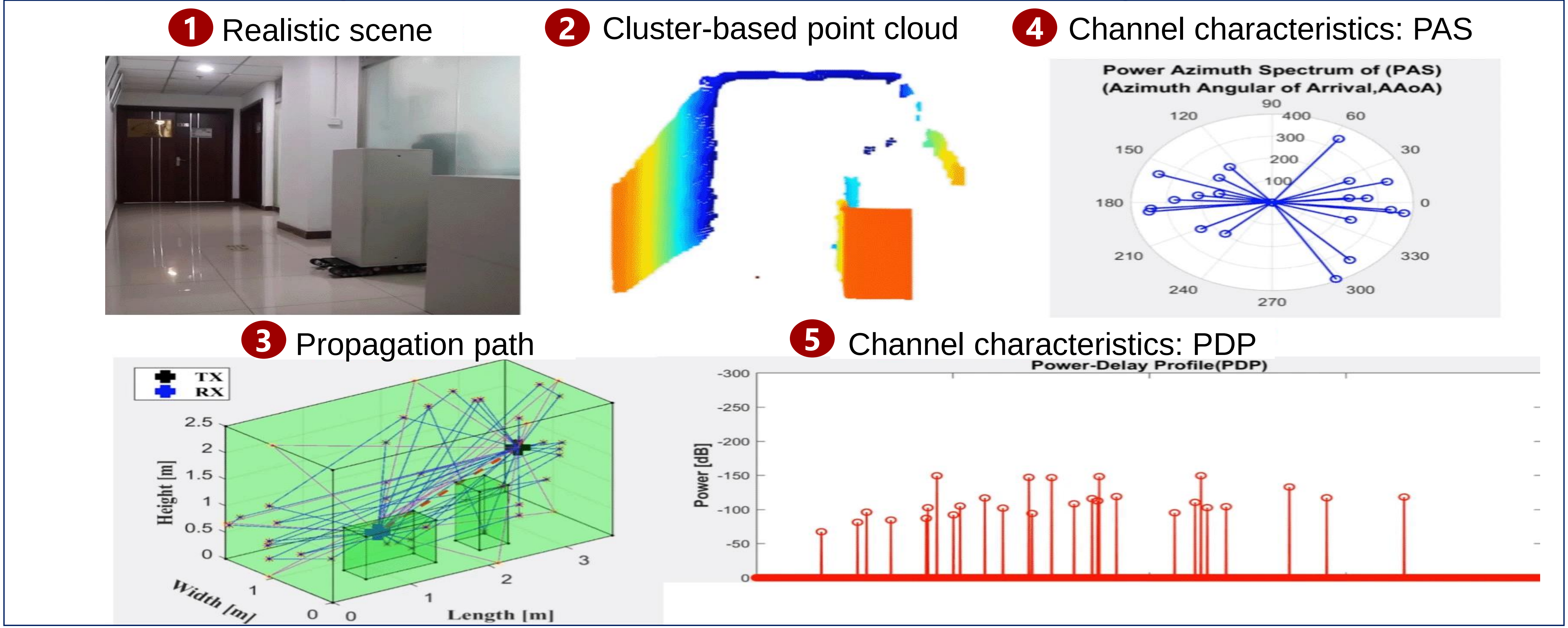

- Y. Miao, Y. Zhang, J. Zhang, et al., *"Demo Abstract: Predictive Radio Environment for Digital Twin Communication Platform via Enhanced Sensing," IEEE Conference on Computer Communications Workshops, 2023, accepted.*

4.5 Platform 2: RIS channel simulator

- Simulations for multi-scenarios, multi-bands, and multi-antennas are supported.

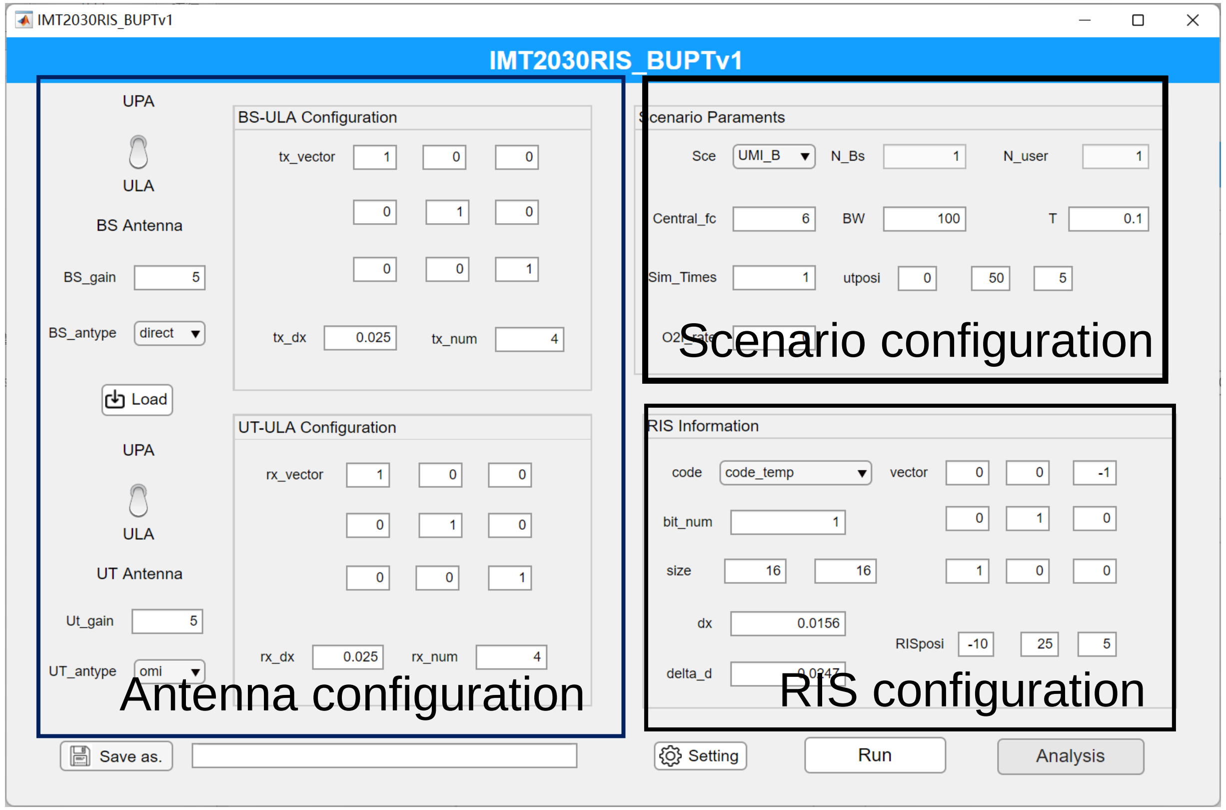

Configuration	Type
Antenna	ULA/UPA
Scenario	UMa/UMi/RMa/InH/O2I
Frequency	CM wave/MM wave/THz
RIS	Position/codebook/scattering model/size/number of elements

- *BUPTCMG-IMT2030_RIS simulation tool. (Platform address: http://www.zjhlab.net/publications/buptcmg-imt2030_ris/)*

- *H. Gong, J. Zhang, Y. Zhang, et al., "How to Extend 3D GBSM Model to RIS Cascade Channel with Non-ideal Phase Modulation?," arXiv preprint arXiv:2302.07501, 2023*

Outline

I. Trend and vision to 6G channel model

II. Our recent progress on 6G channel research

- Terahertz channel measurement and modeling
- Joint communication and sensing channel measurements and modeling
- Massive MIMO channel measurements and modeling
- Intelligent channel modeling and channel prediction

III. Work on 6G channel model standardization

Timeline of 5G and 6G standardization work

- At present, it is in the key stage of the standardization of the 6G channel model!

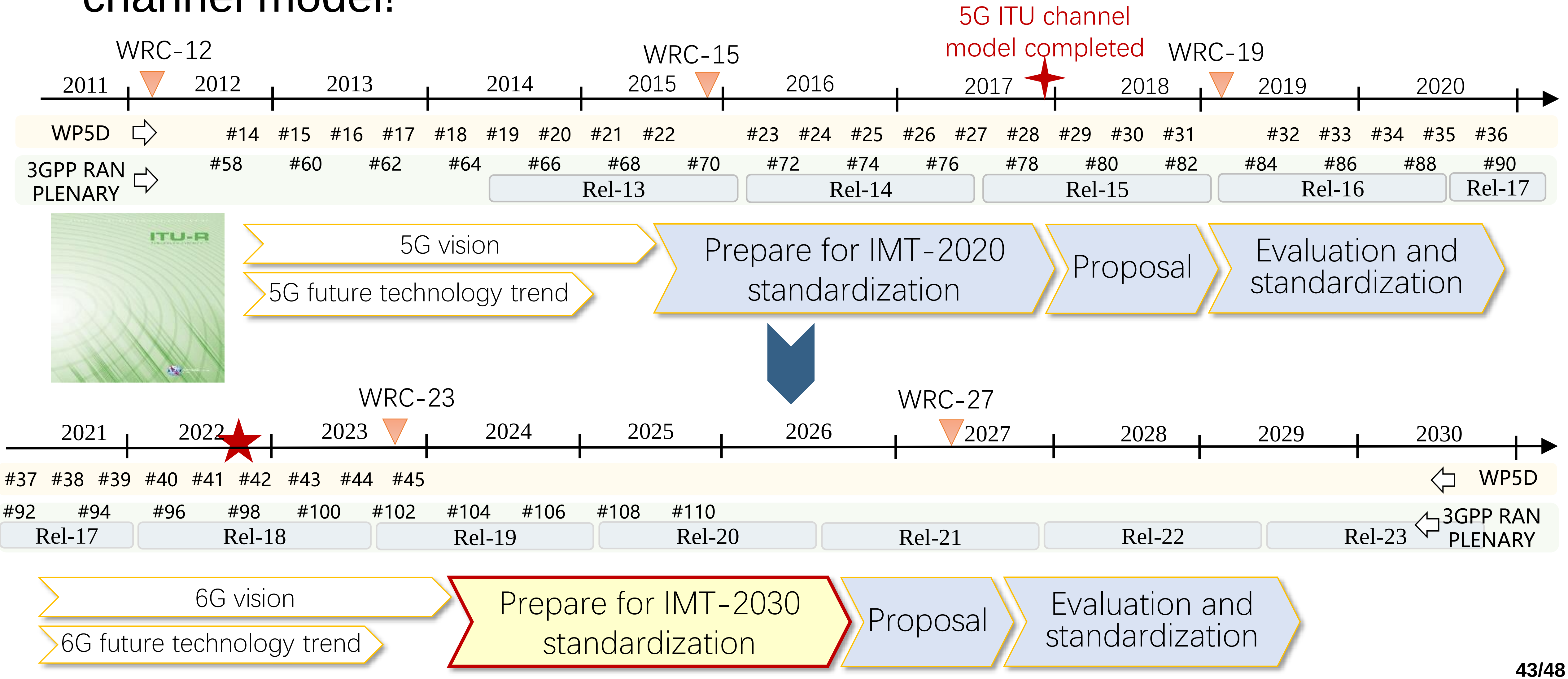

6G channel measurement and modeling task group

- China has established an official channel measurement and modeling task group dedicated to 6G channel research and standardization.

Initiator
The Ministry of Industry and Information Technology
Administrator
The China Academy of Information and Communications Technology

	Chairwoman	Deputy Chairman			
Affiliation	Beijing University of Post and Telecommunica-tions	Huawei Technologies Co., Ltd	Zhongxing Telecom Equipment	China Mobile	China Academy of Information and Communication-s Technology
Name	Jianhua Zhang	Jian Li	Jianwu Dou	Liang Xia	Hui Liu

Over 35 members from universities, enterprises, research institutes, etc.

White paper on channel measurement and modeling for 6G

- The white paper on channel measurement and modeling for 6G was released at the Global 6G Development Conference.

- **THz communication channel research**
  - THz communication channel measurement platform and scenario
  - THz communication channel characteristics analyze
- **VLC channel research**
  - VLC channel pass loss model
  - Geometry-based 3D space-time-frequency Non-Stationary Channel Model for 6G indoor VLC systems
  - Indoor Visible Light Communication Systems
  - VLC channel noise analysis
- **JCAS channel research**
  - JCAS channel modeling scenarios and requirements
  - JCAS channel measurement and simulation research
  - JCAS channel modeling method research
- **RIS channel research**
  - RIS channel model
  - Simulation and measurement of RIS channel model
- **New channel modeling methods**
  - Universal geometry-based stochastic channel model for 6G
  - Map-based hybrid channel model
  - Cluster-Nuclei Based Channel Model
  - Hybrid ray and graph channel model

Download address: https://www.imt2030.org.cn/html//default/zhongwen/chengguofabu/yanjiubaogao/index.html?index=2

Thanks for your attention and welcome your comments!

Related publications

1. J. Zhang et al., *“Channel Measurements and Models for 6G: Current Status and Future Outlook,” Frontiers of Information Technology & Electronic Engineering, 2020.*

2. J. Zhang et al., *“3D MIMO: How Much Does It Meet Our Expectation Observed from Antenna Channel Measurements?”, IEEE Journal on Selected Areas in Communications, 2017.*

3. *P. Tang,* J. Zhang, *et.al., “Channel Measurement and Path Loss Modeling from 220 GHz to 330 GHz for short-range wireless communications”, China Communications, 2021.*

4. *Z. Chang,* J. Zhang, *et.al., "Frequency-Angle Two-Dimensional Reflection Coefficient Modeling Based on Terahertz Channel Measurement," Frontiers of Information Technology & Electronic Engineering, accepted.*

5. *ITU-R Document 5D/1640-E, “Proposal on the Development of Preliminary Draft New Report,” 43th Meeting of Working Party 5D, E-Meeting, 2023.*

6. J. Zhang, *J. Lin, P. Tang, W. Fan, X. Liu, Z. Yuan, H. Xu, Y. Lyu, L. Tian and P. Zhang, "Deterministic Ray Tracing: A Promising Approach to THz Channel Modeling in 6G Deployment Scenarios," IEEE Communications Magazine, accepted.*

7. *X. Liu, J. Zhang, P. Tang, L. Tian, H. Tataria, S. Sun, M. Shafi , “Channel Sparsity Variation and Model-Based Analysis on 6, 26, and 132 GHz Measurements”, arXiv preprint arXiv: 2302.08772 , 2023.*

8. *J. Wang,* J. Zhang, *Y. Zhang et al., “Empirical Analysis of Sensing Channel Characteristics and Environment Effects at 28 GHz,” IEEE GLOBECOM Workshops, 2022.*

9. *Y. Liu,* J. Zhang, *Y. Zhang, Z. Yuan, G. Liu , “A Shared Cluster-based Stochastic Channel Model for Joint Communication and Sensing Systems”, arXiv preprint arXiv: 2211.06615, 2022.*

10. *Z. Yuan,* J. Zhang, *Y. Ji, G. Pedersen, and W. Fan, "Spatial Non-stationary Near-field Channel Modeling and Validation for Massive MIMO Systems, " IEEE Transactions on Antennas and Propagation, 2022.*

11. J. Zhang, *Y. Zhang and L. Yu et al., "3-D MIMO: How Much Does It Meet Our Expectations Observed From Channel Measurements?," in IEEE Journal on Selected Areas in Communications, 2017.*

12. J. Zhang, *et al., “A deterministic channel modeling method for RIS-assisted communication in sub-THz frequencies,”17th European Conference on Antennas and Propagation (EuCAP), 2023, accepted.*

Related publications

13. H. Gong, J. Zhang, Y. Zhang, et al., "How to Extend 3D GBSM Model to RIS Cascade Channel with Non-ideal Phase Modulation?," arXiv preprint arXiv:2302.07501, 2023.

14. J. Zhang, "The interdisciplinary research of big data and wireless channel: A cluster-nuclei based channel model," China Communs, 2016. (First Best Paper Award)

15. L. Yu, Y. Zhang, J. Zhang, Implementation framework and validation of cluster-nuclei based channel model using environmental mapping for 6G communication systems, China Communs, 2022.

16. Y. Sun, J. Zhang, Y. Zhang et al., "Environment Features-Based Model for Path Loss Prediction," IEEE Wireless Communications Letters, 2022.

17. Y. Sun, J. Zhang, et al., "How to Define the Propagation Environment Semantics and Its Application in Scatterer-Based Beam Prediction," IEEE Wireless Communications Letters, 2023, early access.

18. G. Nie, J. Zhang, et al., "A Predictive 6G Network with Environment Sensing Enhancement: From Radio Wave Propagation Perspective" China Communications, 2022. (COVER ARTICLE)

19. X. Chen, L. Tian, P. Tang and J. Zhang, "Modelling of Human Body Shadowing Based on 28 GHz Indoor Measurement Results," 2016 IEEE 84th Vehicular Technology Conference (VTC-Fall), 2016.

20. G. R. MacCartney, T. S. Rappaport and S. Rangan, "Rapid Fading Due to Human Blockage in Pedestrian Crowds at 5G Millimeter-Wave Frequencies," GLOBECOM 2017 - 2017 IEEE Global Communications Conference, 2017.

21. L. Yu, J. Zhang, Y. Zhang, et al., "Long-Range Blockage Prediction Based on Diffraction Fringe Characteristics for mmWave Communications," IEEE Communications Letters, 2022.

22. Y. Miao, Y. Zhang, J. Zhang, et al., "Demo Abstract: Predictive Radio Environment for Digital Twin Communication Platform via Enhanced Sensing," IEEE Conference on Computer Communications Workshops, 2023, accepted.

23. H. Gong, J. Zhang, Y. Zhang, et al., "How to Extend 3D GBSM Model to RIS Cascade Channel with Non-ideal Phase Modulation?," arXiv preprint arXiv:2302.07501, 2023